Master of Science dissertation:

Utilizing statistical process control analysis and EPID for routine QA of medical linear accelerators

Patrik Andersson

Supervisors:

Claus F. Behrens, PhD

Ulf Bjelkengren

David Sjöström

This work has been carried out at the Department of oncology, Copenhagen University Hospital, Herlev, Denmark

Department of Medical Radiation Physics, Clinical Sciences, Lund
Lund University, Sweden, 2011

Patrik Andersson, Master of Science Dissertation: *Utilizing statistical process control analysis and EPID for routine QA of medical linear accelerators*, spring 2011.

Acknowledgements

First of all, I would like to thank all the people at Herlev University hospital involved in this work for their help and support.

Special thanks to:

- Claus F. Behrens for his many ideas which helped me improve my Master of Science dissertation,

- Ulf Bjelkengren for always being there and for supporting me when I needed it the most and

- David Sjöström for giving me all the motivation and inspiration I needed to accomplish this work.

I would also like to acknowledge the following foundations for making it possible for me to continue develop my research and to present my results at the 2011 joint AAPM/COM meeting in Vancouver (see abstract, accepted for poster presentation, in Appendix V):

- Stiftelsen Regementsläkaren dr Hartelii stipendiestiftelse

- John och Augusta Perssons stiftelse

- Novartis

A popularized summary in Swedish:

Strålbehandlingsapparatens inbyggda kontrollant

Strålbehandling är en vanlig behandlingsform av cancer. Tumören bestrålas med röntgenstrålning med hög energi. Vid strålbehandling av cancer är det av stor vikt att frisk vävnad inte utsätts för onödig strålning, samtidigt som stråldosen till cancercellerna ska vara tillräckligt hög för att döda tumören. Därför är det även viktigt att de apparater (lineäracceleratorer) som används för behandlingen ger strålning som håller önskvärd kvalitet.

För att säkerställa att strålbehandlingsapparaterna levererar strålning av god kvalitet genomförs regelbundna kvalitetskontroller med hjälp av olika sorters utrustning beroende på vilken egenskap hos strålningen man är intresserad av. En gemensam faktor för den största delen av den här typen av utrustning är att det krävs att användaren ställer upp utrustningen i rätt position med hjälp av lasrar och distansverktyg. Mätningarna resulterar ofta i ett värde, på någon egenskap hos strålningen från acceleratorn, vars avvikelse från ett referensvärde måste ligga innanför vissa gränser.

Ett mer användaroberoende alternativ skulle kunna vara den bildregistrerande utrustning (så kallad bildplatta) som finns monterad på alla apparater. Bildplattan används vanligen för att ta bilder på patienten för att kontrollera att det är tumörområdet som behandlas och inte omkringliggande frisk vävnad. Bildplattan ger alltså möjlighet att ta bilder i två dimensioner, vilket skulle kunna utnyttjas till kontroller av vissa egenskaper hos strålningen från acceleratorn, i jämförelse med de beprövade mätmetoderna som vanligtvis endast sker i en punkt.

För att undersöka bildplattans lämplighet för kvalitetskontroll av strålbehandlingsapparater samlades det varje behandlingsdag, under cirka tre månader, in bilder (utan patient) med bildplattan. Analys genomfördes för att med hjälp av bilderna bland annat kunna kontrollera röntgenstrålningens energi och stråldosen i förhållande till det önskade. En ny statistisk metod, för att få fram de gränser som de uppmätta värdena måste ligga innanför, testades även. Vad värden uppmätta med bilplattan motsvarade för övrig utrustning kontrollerades och uppföljning med övrig utrustning gjordes vid flera tillfällen under de här tre månaderna.

Resultaten visar att bildplattan har stor potential att kunna utnyttjas som utrustning för kontroll av strålbehandlingsapparater. I själva verket visade den bättre resultat än den utrustning som tidigare utnyttjats för daglig kontroll av stråldosen. Samtidigt innebär utnyttjandet av bildplattan att extra information om bland annat strålningens energi kan fås. Gränserna som togs fram med den nya statiska metoden gav goda indikationer på när strålbehandlingsapparaten inte fungerade som den skulle och bidrog till att ge personalen mer tid på sig att genomföra justeringar innan det blev kritiskt.

Handledare: Claus F. Behrens, Ulf Bjelkengren och David Sjöström.
Examensarbete på 30 hp i medicinsk strålningsfysik, vårterminen 2011
Avdelningen för medicinsk strålningsfysik, Lunds universitet
Arbetet utfördes på universitetssjukhuset i Herlev, Danmark

Abstract

Purpose: The main purposes of this study is to a) evaluate the suitability of a Varian aS1000 EPID as a safe quality assurance device for control of machine specific parameters, such as linac output, beam quality and beam symmetry, and b) to investigate the usefulness of the SPC concept for evaluation of the obtained data.

Method and Materials: Measurements were performed using a Varian Clinac 2300iX linear accelerator (Varian, Inc., Palo Alto, CA, USA), equipped with an a-Si EPID (Varian a-Si1000). The suitability of the EPID as a device for daily quality control of the linac output was investigated for 6 MV and 15 MV. The EPID measurements were compared to Linacheck (PTW GmBh, Freiburg, Germany) as well as ionization chamber measurements in water (NE2571 farmer type ionization chamber, NE Technology Ltd., Reading, UK). The ability of an a-Si EPID to verify the beam quality and beam profile parameters was investigated by adjustments of the bending current shunt voltage and the steering current, respectively. A MATLAB© script was developed for analysis of the acquired EPID images. Statistical process control (SPC) was applied on the daily measurements and obtained action levels were compared to fixed limits and the standard deviation of the data.

Results: The linear response of the EPID with varying number of monitor units (r^2=0.999) made it suitable for detection of output deviations during the daily measurements. These detected deviations could be confirmed as true deviations by follow-up measurements using both the Linacheck as well as ionization chamber. The SPC provide determination of the stability of the process. A drift in the linac output was for example detected by the SPC analysis, indicating an unstable process. Adjustments of the beam quality and symmetry could be readily detected by the a-Si EPID and was traceable to water measurements and data collected during commissioning of the linac. A deviation of 0.3% in the TPR measured in water corresponded to a 0.5% change in the hump measured with EPID.

Conclusion: The EPID is suitable as a device for daily quality control of linac output. The user independence and the flexibility of the EPID as a two-dimensional detector are the main advantages. The latter meaning it can be used for constancy control of beam quality and symmetry. Using SPC provides better knowledge on when to act on varying data points, in comparison to the use of for example fixed limits or to limits obtained by calculating the standard deviation based on a set of data points without any consideration to any time order. The stability of a process can be monitored and it gives a good balance between sensitivity and resources available for corrective actions.

Supervisors: **Claus F. Behrens, Ulf Bjelkengren and David Sjöström.**
Degree project of 30 credits medical radiation physics, spring 2011
Department of Medical Radiation Physics, Lund University, Sweden
The work was carried out at the department of oncology, Copenhagen University hospital, Herlev, Denmark.

Abbreviations and acronyms

2D	Two-dimensional
3D	Three-dimensional
AAPM	American Association for Physics in Medicine
ALARA	As Low As Reasonably Achievable
a-Si	Amorphous Silicon
CU	Calibrated Units
EPID	Electronic Portal Imaging Device
GUI	Graphical User Interface
ICRU	International Commission on Radiation Units and Measurements
IEC	International Electrotechnical Commission
IMRT	Intensity Modulated Radiotherapy
MLC	Multi-Leaf Collimator
MU	Monitor Units
MV	Mega Voltage
NTCP	Normal Tissue Complication Probability
PMMA	Polymethylmethacrylate
RTT	Radiotherapy Technologists
SD	Standard Deviation
SPC	Statistical Process Control
SSD	Source-Skin Distance
TCP	Tumour Control Probability
TPR	Tissue Phantom Ratio
QA	Quality Assurance
QC	Quality Control

Table of contents

1 Introduction

Radiotherapy is an important modality for cancer treatment and it is applied in nearly half of all cancer treatments (1). Since the main purposes of cancer treatment are to cure, relieve patients from pain and help to increase the quality of life, it is of high importance to assure that the treatment delivery is carried out with high accuracy and precision. A high accuracy and precision is also a prerequisite to assure that the complications to the surrounding normal tissue are minimized. A minor change in dose can namely cause a major change in tumour control probability (TCP) and normal tissue complication probability (NTCP) (2). Patient specific quality assurance (QA) and machine specific QA are therefore essential in radiotherapy (Appendix I). In Sweden, recommendations and demands on quality assurance in radiotherapy are given by the Swedish Radiation Safety Authority (3). These rules and recommendations follow those recommendations given by for example the American association of physics in medicine (AAPM) (4). The total uncertainty in radiotherapy is considered by some to be approximately 3% (1 standard deviation, SD) (5) with the demand that for example the uncertainty of dose determination at the calibration point is no more than 1% (1 SD) (Table 1).

Table 1. Determination of accuracy goal in dose calculation carried out by Ahnesjö et al. (1999) with the uncertainties under future development being the requirements on the radiotherapy of today.

	Present technique 100 x ΔD(1SD)/D	Future development 100 x ΔD(1SD)/D
Absorbed dose determination at the calibration point	2.0	1.0
Additional uncertainty for other points	1.1	0.5
Monitor stability	1.0	0.5
Beam flatness	1.5	0.8
Patient data uncertainties	1.5	1.0
Beam and patient set-up	2.5	1.6
Overall excluding dose calculation	**4.1**	**2.4**
Dose calculation	1.0 2.0 3.0 4.0 5.0	0.5 1.0 2.0 3.0 4.0
Resulting overall uncertainty	**4.2 4.6 5.1 5.7 6.5**	**2.4 2.6 3.1 3.8 4.7**

To assure that the accuracy lies within the recommendations mentioned above, the quality of the devices used for quality control (QC) of the linear accelerator machine specific parameters need to be adequate, for example regarding its uncertainties. The choice of the QC device is often also based on the flexibility of the device. A device with multiple purposes and a device that is time efficient (low demands on resources) is beneficial. This is perhaps why some studies have investigated the ability of electronic portal imaging devices (EPIDs) to act as dosimetric quality assurance device (6; 7; 8; 9) (Appendix II). The use of an EPID, mounted directly on the linear accelerator, for QC would probably decrease the set-up uncertainty since it is automatically positioned without having the user (or multiple users) align the device by lasers and distance indicators. It could also render in a more time efficient procedure than using other more cumbersome devices like for example a scanning diode in water for beam profile measurements. Previous studies indicate that images acquired with an EPID could be used for monitoring of linear accelerator parameters such as output and beam symmetry (8). Most studies regarding the EPID as a device for quality assurance have however been carried out on accelerators from ELEKTA (Elekta Oncol-

ogy Systems, Crawley, UK) and there is a need for investigation of the ability of Varian (Varian, Inc., Palo Alto, CA, USA) a-Si EPIDs to act as quality assurance devices.

An important aspect of the quality assurance process is the calculation of so-called action limits. These limits are calculated with the purpose to act as a limit, outside of which an action is required. Quality assurance in radiotherapy is often like monitoring a process by collecting data over a long period. The use of an analysis more focused on an iterative process over time to obtain action limits, rather than using fixed limits or limits based on for example only the standard deviation of the collected data, is compelling. One concept, which has been suggested (10), is the so-called statistical process control (SPC) analysis (Appendix III).

The main purposes of this study is to a) evaluate the suitability of a Varian aS1000 EPID as a safe quality assurance device for control of machine specific parameters, such as linac output, beam quality and beam symmetry, and b) to investigate the usefulness of the SPC concept for evaluation of the obtained data.

2 Materials and methods

All measurement were carried out using a Varian Clinac 2300iX linear accelerator (Varian, Inc., Palo Alto, CA, USA), equipped with an a-Si EPID (amorphous silicon EPID, Varian aS1000) (Figure 1). Description of the a-Si EPID is presented elsewhere (Appendix II).

Figure 1. Varian Clinac 2300iX linear accelerator equipped with an a-Si EPID.

Measurement devices, abbreviations used in this report, manufacturer and the purposes with the measurements are presented in Table 2.

Table 2. Measurement devices, abbreviations used for the corresponding devices, their manufacturers and to what purpose they have been utilized during this study.

Device	Abbr.	Manufacturer	Purpose
Varian aS1000 (a-Si EPID)	EPID	Varian Inc., Palo Alto, CA, USA	Output, beam quality, symmetry
Linacheck (built-in plane parallel ionization chamber + 5 cm additional PMMA build-up)	LC	PTW GmBh, Freiburg, Germany	Output
FC65-P ionization chamber in 20x20x20 cm^3 PMMA phantom	ICPMMA	Scanditronix Wellhöfer, Uppsala, Sweden	Output
NE-2571 ionization chamber in water phantom	ICW	NE technology limited, Reading UK	Output, beam quality
Blue phantom	BP	Scanditronix Wellhöfer, Uppsala, Sweden	Output, beam quality, symmetry
CC13 ionization chamber in BP	ICBP	Scanditronix Wellhöfer, Uppsala, Sweden	Output, beam quality, symmetry
PFD-3G diode in BP	DBP	IBA dosimetry, Uppsala, Sweden	Output, beam quality, symmetry
Starcheck (2D multi-array ionization chamber detector + 5 cm RV3 build-up + 5 cm RV3 backscatter)	SC	PTW GmBh, Freiburg, Germany	Output, beam quality, symmetry

Before making use of the EPID it was calibrated by acquiring a dark field as well as a flood field (field size of 40.2 x 32 cm^2, covering the entire active area). A dosimetric calibration was also carried out. After measurement of a 100 MU beam with an ionization chamber in water (ICW) and a field size of 10 x 10 cm^2, the signal detected with the EPID for a similar beam was normalized to give a signal (in calibrated units, CU) corresponding to the deviation from the reference as detected with the ionization chamber. This was carried out for all beam qualities and dose rates. It should be noted that a correction of the linac output should always be followed by an EPID calibration.

2.1 Feasibility tests

2.1.1 Linearity

Knowledge of the relationship between detected output and the actual delivered dose is essential for every device, used for quality control of linear accelerator output, to secure that the delivered dose to the patient lies within the clinical tolerance. A linear relationship between specified number of monitor units (MU) and detected output is desirable, e.g. as the one for ionization chamber. The linearity of the EPID was investigated in the interval between 95 and 105 MU in steps of 1 MU, since most of the study was to be carried out with fields of approximately 100 MU. The linearity test was however expanded to monitor units ranging from 5 up to 350. The linearity was also investigated for an ionization chamber (ICW) at a depth of 10 cm in water as well as the Linacheck (LC) in the interval between 95 and 105 MU. The linearity was tested for field size 10 x 10 cm^2 at SSD 100 cm (central pixel in isocenter). To be able to compare the different measurement devices the detected signal was normalized to a relative dose of 100% for a specified number of monitor units (100).

2.1.2 Ghosting

Previous reports regarding dosimetric properties of a-Si EPIDs have reported effects of so-called ghosting (11; 12). Ghosting refers to the changed pixel sensitivity that occurs due to trapped charge, which alters the electric field strength in the bulk or surface of the photodiode layer (11). The extent of the effect has been proven to depend on the exposure time and the time between readout (11; 12). The effect should be separated from the effect called image lag. The image lag effect of an a-Si EPID occurs when trapped charge is read out in a subsequent frame, resulting in an off-set in the EPID signal (11). Most of the reports, however, concern the predecessor to the Varian aS1000, namely the Varian aS500, and therefore the extent of the ghosting effect was tested on the EPID used during this study. When testing the ghosting effect the result will be a combination of the image lag as well as ghosting (11). To test the ghosting effect on the Varian aS1000 it was initially irradiated with 500 MU and a field size of 5 x 5 cm^2. This relatively small field was, immediately after completion, followed by an irradiation with 100 MU and a field size of 10 x 10 cm^2. Although the second image was acquired "immediately" after the first field, the time between the two fields was in the order of 20 seconds. This, however, was the minimum time that elapsed between two successive measurements during the rest of this study. Therefore the result will give a good indication of how great of impact the ghosting effect will have and if any corrections for the effect must be carried out.

2.2 Adjustment of beam quality and symmetry

2.2.1 Beam quality

The ability of the EPID to detect deviations in photon beam quality was investigated by adjusting the bending current shunt voltage. By altering the current to the 270-degree bending magnet power supply a filtration of photon energy is possible. Measurements of the beam quality are often carried out by collecting depth ionization curves and calculating the $TPR_{20/10}$ (tissue phantom ratio). A change of the bending current shunt voltage will however, in addition to the change of $TPR_{20/10}$, also affect the horns on the beam profile. For example a decrease of the bending current shunt voltage, implying a decrease in beam quality, will raise the horns on the profile. The horns are present in photon beams because of the flattening filter. The flattening filter is used to create a flat dose profile at a particular depth, which will render in horns with higher dose at more shallow depths. These horns are dominated by absorbed dose from low energy photons, and decreasing the average energy of the photon beam will cause the dose in the horns to increase. The opposite, lowered horns, will appear when the average photon energy is instead increased. The possibility to extract the beam profile from the acquired 2D EPID images can be used to detect changes in the beam profile dose horns and therefore also the beam quality.

Initially reference data was collected. The reference data for beam quality (depth ionization curves) were obtained with a CC13 ionization chamber (ICBP) placed in a 3D water phantom (Blue phantom, BP) and the beam profile was obtained using a PFD-3G diode (DBP) in the same water phantom. The TPR was obtained from the depth ionization curves. Further, reference data was collected with the EPID and also with Starcheck (SC). Reference data is, in this case, the data collected before adjustments of any parameters on the linear accelerator (no data was acquired for the EPID and Starcheck during commissioning). During this experiment Starcheck acted as a device to quickly ensure that the deviations obtained were as intended, before measurements were done with the more cumbersome 3D water phantom. In addition to this, the Starcheck measurements were also compared to the EPID and the water phantom measurements. The reference data consisted of beam quality data as well as beam profile data. To be able to trace the measurements back to the commissioning, beam profile was measured with a diode in the 3D water phantom using a 40x40 cm^2 field size which was used during commissioning. Since this field size exceeded the maximum field size when measuring with the EPID at a SSD of 100 cm measurements were also carried out using field sizes of 25x25 cm^2 as well as 10x10 cm^2.

The process of altering the beam quality is fairly cumbersome, since an adjustment of the bending current shunt voltage was obtained by manually adjusting a potentiometer in the auxiliary electronic chassis, located on the linac stand. Therefore, to assess at which bending current shunt voltage a significant change in beam quality would appear, the Starcheck was used. Using the Starcheck is a much faster process than using the Blue phantom water phantom for measurement of a depth ionization curve. The reference bending current shunt voltage on the potentiometer was measured to be 13.5 mV for 6 MV and was initially changed to 12.5 mV. This change, however, caused the dose rate to fluctuate and could not be used. The bending current shunt was altered until a stable dose rate was reached at 13.0 mV. A similar process for 15 MV resulted in a

change of bending current shunt from 34.0 mV to 33.0 mV. Measurements were carried out with the Starcheck for both energies and a field size of 25x25 cm^2. With the same changes in bending current shunt voltage, images were acquired with the EPID, using field sizes of 10x10 cm^2 and 25x25 cm^2 for both 6 MV and 15 MV and the depth ionization curve and also the beam profile were measured in the water phantom. The choice of only measuring one decrease in energy was made because of lack of time and the fact that a decrease in energy would mean an increase in the profile horns. An increase in energy, which would result in lowered horns, would be harder to detect since the beam profile in its original appearance is quite flattened to start with.

After the initial adjustment of the bending current shunt voltage, further investigation of the ability of the EPID to detect deviations in beam quality was carried by utilizing the SC, the EPID and an ionization chamber in a water phantom (ICW), where the latter only was used to calculate the $TPR_{20/10}$ (13). The bending current shunt was stepwise altered from 13.0 mV up to 14.3 mV for 6 MV (from 33.0 mV up to 35.5 mV for 15 MV). Measurements were carried out with the Starcheck, the EPID as well as the ionization chamber for all bending current shunt voltage adjustments, making it possible to evaluate the ability of the EPID to detect an increase as well as a decrease in the photon beam quality.

Measurements were performed again after the bending current shunt voltage was brought back to the reference value. The standard deviation of the measurements at the reference conditions (before and after all adjustments) was obtained and used as an indication of the uncertainty.

All evaluation of the acquired EPID images, extraction of beam profiles and calculations of beam quality parameters was carried out off-line with a script written in MATLAB (MATLAB 7.5, The MathWorks Inc., Natick, MA, 2000). Evaluation of the acquired EPID images to assess the beam quality was carried out by calculating the so-called hump. Calculation of the hump value can be used for assessment of the deviation in the beam profile horns. It is known that a decrease in energy will cause the horns to rise above the reference position of the beam profile and vice versa for an increase in energy. To use this fact in analyzing the EPID images the hump was calculated, according to the International Electrotechnical Commission (IEC) (14), as

$$\text{Hump} = \frac{\left(D_{R,\max} + D_{L,\max}\right)}{2 \cdot D_C}, \qquad \text{(Eq. 1)}$$

Where $D_{R,\max}$ and $D_{L,\max}$ are the right and left extreme values of the flattened area and D_C is the signal at the beam centre. The flattened area is defined as 90% of the area corresponding to the 50% dose level (for field sizes ≤30 cm). The hump was also calculated for the starcheck measurements and values from EPID as well as starcheck measurements were compared with TPR values obtained from measurements in the water phantom.

2.2.2 Beam symmetry

The procedure of investigating the ability of the EPID to detect deviations in beam symmetry was similar to that for beam quality deviations. This investigation was, however, not as thorough

as the one for beam quality. Reference data for the EPID, the SC and a scanning diode (DBP) in a 3D water phantom was initially collected.

Adjustment of the steering current was carried out to obtain asymmetric beam profiles. The procedure of adjusting the steering current is somewhat cumbersome and this investigation was therefore only carried out for 6 MV and a field size of 25x25 cm^2. The field size often used for daily monitoring of the beam output, however, is 10 x 10 cm^2. Therefore the ability of the EPID to detect deviations in beam profile symmetry for that field size was also investigated.

To adjust the photon beam profile the dosimetry system was bypassed. In this way a change in symmetry that normally would have triggered an interlock on the machine was reachable. The steering current was only adjusted to a level (±2%) at which point the interlock would normally intervene. This was, for example, obtained when the T-sym (transverse symmetry) parameter was adjusted to -2.2, as in this study, corresponding to a 2.2% change in the symmetry. Measurements at the adjusted steering current were carried out using the EPID, the Starcheck as well as the scanning diode. The visible evaluation of the beam profiles was combined with calculation of the beam symmetry (14) according to equation 2, resulting in a value of 100% for perfect symmetry.

$$Symmetry = \left(\frac{D_L}{D_R} \right)_{\max} \cdot 100 \qquad \text{(Eq. 2)}$$

D_L and D_R are the left and right values at equal distance from the beam centre, respectively. The maximum value of the ratio between these values, within the flattened area, times 100 is defined as the symmetry in percent.

2.3 Daily quality control tests

Four images were acquired each day during approximately three months, with the exception of occasional missed days, weekends and service days. The total number of measurement occasions was 58. Two images were acquired with 100 MU for 6 MV and 15 MV respectively, one with a 10 x 10 cm^2 field size and the other with a 25 x 25 cm^2 field size. All images were acquired with a collimator angle of 0°, a gantry angle of 0° and without any additional build-up. For comparison the output was also measured with the routinely used Linacheck before patient treatment every day. This measurement was carried out by placing the Linacheck at an SSD of 100 cm, where after an additional build-up layer was placed on top of the Linacheck.

The daily measurements were carried out every morning and, to check the stability of the system, frequent measurements of the linac output were carried out with ICW in the afternoons. Data were also acquired with the EPID and the linacheck in the afternoons, both to observe the drift during the day and to observe how well these devices follow ICW measurements under reference conditions. The EPID was not calibrated during the collection of data, why the comparison between the ionization chamber measurements and the EPID measurements could give an indication of how often the EPID should be calibrated.

A comparison between the EPID system and the system currently in use for weekly quality assurance of the output at the department was also carried out. The system currently in use for weekly output measurements was an ionization chamber (FC65-P, Scanditronix Wellhöfer, Uppsala, Sweden) placed in a PMMA phantom at a depth of 10 cm (ICPMMA).

A so-called student's t-test was carried out, using MATLAB, to compare the EPID with the ICW, the ICPMMA and the LC as well as the LC with ICW. The null hypothesis was that data samples from two devices were independent random samples from normal distributions with equal means and equal but unknown variances. The result of the test was either a rejection of (h=1) or a failure to reject (h=0) the null hypothesis. The result was given with a certain probability (the p-value), under the null hypothesis, of observing a value as extreme or more extreme of the test statistic $t = \bar{x} + \bar{y} \Big/ \sqrt{s_x^2/n + s_y^2/m}$, where $\bar{x}$ and $\bar{y}$ are the sample means, s_x and s_y the sample standard deviations and n and m are the sample sizes. If nothing else is stated, the significance level for all t-tests is α=0.05.

Evaluation of the linac output measured with EPID was carried out off-line, by calculating an average of the central 21 x 21 pixels, corresponding to an area of approximately 0.82 x 0.82 cm^2, for both field sizes. All data processing was undertaken using a commercial software package (MATLAB 7.5, The MathWorks Inc., Natick, MA, 2000), in which the resulting data was further analyzed by applying statistical process control analysis (see appendix III).

One of the main focuses of this study was to utilize statistical process control (SPC) for analysis and calculation of action limits. Statistical process control analysis is utilizing control charts where systematic variation can be distinguished from random variation (see appendix III for further information about SPC). First of all SPC analysis on the daily measurements renders in a so-called average chart. Data collected in a manner like the daily measurements mean that each subgroup only contains one data point. Therefore every subgroup average equals that value. In addition to these subgroup averages and the standard deviation of the subgroup averages the obtained action limits are also based on the so-called range. The range is, in the case of collecting one data point at a time, the difference between two consecutive measurements. The action limits for the average chart is then calculated according to equations 12 and 13. In the case of the EPID measurements the SPC limits were based on the 20 first data points. The reason for this was that the 21st data point was outside the limits calculated from the 20 first data points. The theory of SPC says that the number of data points used for calculation of the limits can be increased only if the data points of interest lies within the limits obtained with the use of the preceding values (10). The daily EPID and Linacheck measurements are therefore presented together with the limits as well as the mean of the subgroup averages based on the twenty first data points. With values lying inside the SPC limits, and if those limits are within the clinical limits, the system in considered stable and no action is necessary. A process with values ending up outside the SPC limits is considered instable and corrective action to eliminate the cause of the variation should be recommended. Another advantage of utilizing SPC instead of fixed limits is the range chart. Range charts are obtained by calculating the difference between two consecutive data points and give an indication of the variation in output from one treatment day to another.

The two-dimensional EPID images, acquired on a daily basis, were also analyzed to control the constancy of beam quality and beam symmetry. Calculation of beam quality and extraction of beam profile parameters from the acquired EPID images was carried out in the same manner as in section 2.3 (Adjustment of beam quality and profile). Calculation of the hump and the symmetry values of the profiles give the opportunity to utilize statistical process control for analysis and obtaining action limits.

3 Results and discussion

Results presented in this section are all for a beam quality of 6 MV. The corresponding measurements, yielding similar results, carried out for 15 MV are presented in Appendix IV.

3.1 Feasibility tests

3.1.1 Linearity

Measurements with the Varian aS1000 EPID for monitor units varying between 95 and 105 resulted in a highly linear response (Figure 2). The response was also linear when expanded to between 5 MU up to 350 MU (Figure 2c). When comparing EPID measurements with ionization chamber (ICW) measurements in water it can be concluded that they have similar response for varying dose (Figure 2b). The Linacheck (LC), used for daily output measurements, has a response similar to the two other devices (Figure 2a).

The fact that the response of the EPID was highly linear (r^2=0.999) with varying number of monitor units indicates that it can be considered suitable for detection of deviations in for example output for daily quality assurance.

The gradient of the EPID measurements does not differ greatly from that for the ICW measurements. The test therefore proves that the EPID data points are linear with dose within this dose range and that the gradient is adequate to resolve discrepancies in linac output.

The ionization chamber used in this comparison is used for absolute measurements of the linear accelerator output. This means that the EPID is comparable and traceable to a device which is well calibrated and known to have a high accuracy in detecting deviations in linac output.

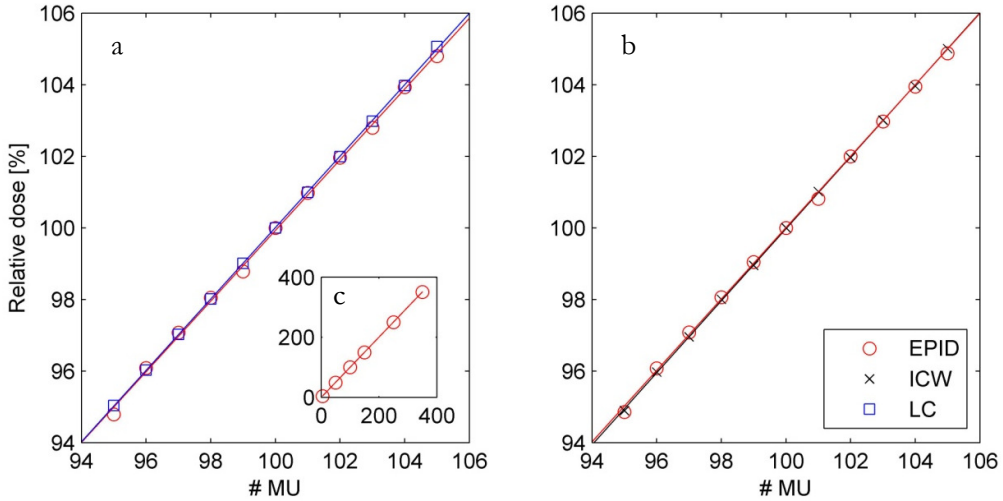

Figure 2. Response of different detectors for varying number of MUs. a) Comparison of EPID and the Linacheck for 95 to 105 MUs. b) Comparison of EPID and an ionization chamber in water for 95 to 105 MUs. c) Response of the EPID for 5 to 350 MUs.

3.1.2 Ghosting

An increase of the detected output was visible within an area of 5x5 cm^2 in the image visualizing the difference between the standard image and the image following irradiation with 500 MU (5x5 cm^2) (Figure 3a). The crossline profile over the image of the difference between the two exposures also visualizes the ghosting effect (Figure 3b). The ghosting effect is, however, only seen as an increase in the order of $1 \cdot 10^{-3}$ CU (Figure 3b). An increase of this magnitude could have an impact on a standard image (100 MU) where the detected output normally is in the order of 1 CU, but not big enough to indicate that the function of the linac could be questioned. Therefore, based on these results, the ghosting effect was considered negligible for the current linac and no correction was made for this during the rest of the study. It should be mentioned that this ghosting effect occurred when the time between the smaller and bigger field was about 20 seconds. This was the shortest time possible between the two fields when making the exposure in clinical mode. No ghosting was detected in the images collected during the rest of this study.

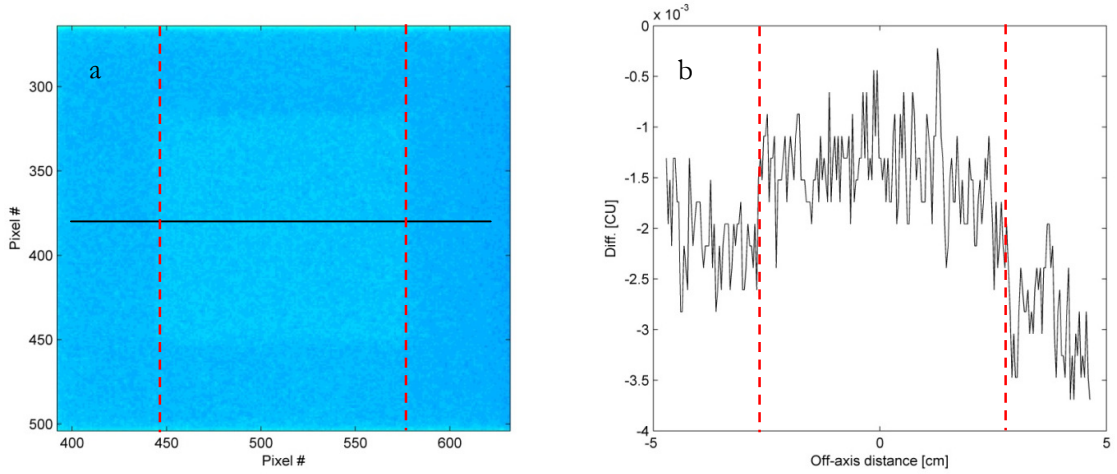

Figure 3. Ghosting effect visualised as a) an image of the difference between a standard exposure of 100 MU (10 x10 cm^2) and a similar exposure following irradiation of the EPID with 500 MU (5x5 cm^2) and b) a crossline profile over that image.

3.2 Adjustment of beam quality and symmetry

3.2.1 Beam quality

Adjusting the bending current shunt voltage, stepwise, from 13.0 mV up to 14.3 mV for 6 MV resulted in visible changes in the beam profile horns for the acquired EPID images (Figure 4a). The corresponding profiles for the SC are presented in Figure 4b. A clear separation between the profile for the smallest adjustments made on the bending current shunt voltage and the reference profile is visible if studying these beam profiles. This, smallest adjustment, corresponds to approximately a 0.2 mV change in bending current shunt voltage in the case of 6 MV. The corresponding change in $TPR_{20/10}$ (ICW) was approximately 0.3%, lying well within the clinically accepted deviations in beam quality of 1% (15). Quantification of the change in beam quality using the hump, based on the EPID beam profiles, according to equation 1 are presented in Table 3 for 6 MV. In the same table values of hump obtained with the SC and values of $TPR_{20/10}$ obtained with an ICW are presented for comparison.

Depth ionization curves (ICBP) and beam profiles (DBP) obtained using the Blue Phantom are presented, for the reference conditions and a bending current shunt voltage of 13.0 mV and a field size of 25x25 cm^2 in Figure 4d and Figure 4c, respectively. Values on $TPR_{20/10}$ obtained from those depth ionization curves were compared to corresponding hump values for EPID and SC in Table 4.

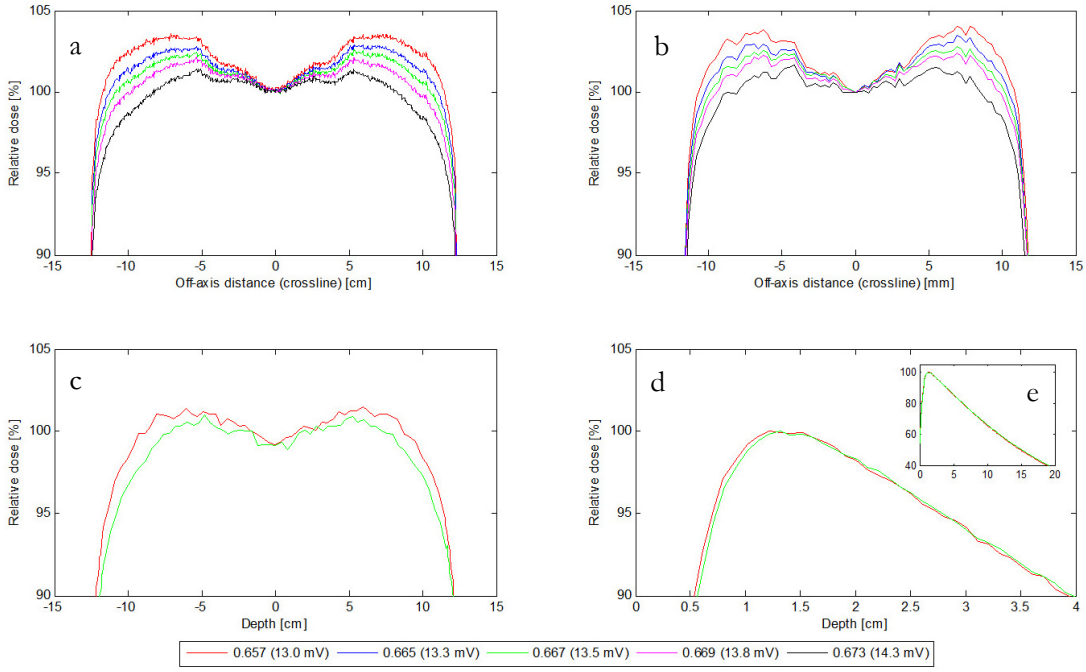

Figure 4. Five different beam profiles, for 6 MV after adjustment of the bending beam quality, acquired with a) the EPID and b) the Starcheck, as well as c) profiles acquired with a diode and the Blue Phantom for the reference beam quality and the lowest bending current shunt voltage and d) depth ionization curves measured with an ionization chamber in Blue Phantom for the same two beam qualities as measured with the diode (e) the two entire depth ionization curves). Legend represents values of $TPR_{20/10}$ (and bending current shunt voltage).

Table 3. Values of TPR20/10 and hump, together with the corresponding deviation from the reference value, obtained with ionization chamber in water (brand), EPID and Starcheck for five different values on the bending current shunt voltage for 6 MV photons.

Bending	ICW		EPID		Starcheck	
current shunt voltage[mV]	$TPR_{20/10}$	Dev.[%]	Hump [%]	Dev.[%]	Hump [%]	Dev.[%]
13.0	0.657	-1.50	97.70	0.96	97.37	0.78
13.3	0.665	-0.30	97.19	0.43	96.04	-0.59
13.5	0.667	0	96.77	0	96.61	0
13.8	0.669	0.30	96.32	-0.46	96.35	-0.28
14.3	0.673	0.90	95.54	-1.27	94.71	-1.97

Table 4. Effects of adjusting the bending current shunt voltage from 13.5 mV to 13.0 mV for 6 MV. The table displays the TPR measured with an ionization chamber (CC13, Scanditronix Wellhöfer, Uppsala, Sweden) in a 3D water phantom (Blue phantom, Scanditronix Wellhöfer, Uppsala, Sweden), the hump measured with EPID and the hump measured with Starcheck.

Measurement device	Blue phantom TPR	EPID Hump [%]	Starcheck Hump [%]
Before adjustment (13.5 mV)	0.669	96.9	95.3
After adjustment (13.0 mV)	0.659	97.7	95.9
Change [%]	-1.5	0.9	0.6

Utilizing the EPID for calculation of the hump as a beam quality parameter will be more sensitive to deviations in the beam quality than the usage of TPR obtained from ionization chamber measurements in water. The sensitivity, however, lies in the same order of magnitude as for the ionization chamber measurements and these results generates a way to relate a deviation in hump detected with the EPID to a deviation in TPR measured with an ionization chamber in water. Thereby a clinical threshold, corresponding to the maximum tolerable deviation measured with an ionization chamber in water, can also be obtained for the EPID. The small deviations in TPR obtained from the adjustments of the bending current shunt voltage also establish the fact that the EPID is fully capable of detecting small deviations in beam quality by extracting the crossline beam profile from an acquired two-dimensional image (Table 3). Note that the standard deviation of the measurements at the reference conditions (before and after all adjustments) was ±0.1% (2SD) for the EPID hump values and ±0.1% (2SD) for the SC hump values. This can be taken as an indication of that the uncertainty in the hump calculation is less than the detected deviations in beam quality. It could, however, be desirable to adjust the bending current shunt voltage in smaller steps to create a more extensive table of the relationship between the hump (EPID) and the TPR (ICW).

As both the values of hump (Table 3) and the beam profiles (Figure 4b) indicates the measurements with the Starcheck are much more uncertain than the EPID measurements, giving for example negative values in hump deviations for positive as well as negative changes in bending current shunt voltage (see Table 7 and Figure 17b in Appendix IV for 15 MV data). This higher grade of uncertainty, in comparison to the EPID measurements where the changes in hump are consistent with changes in bending current shunt voltage, is especially prominent in the beam profiles for 15 MV (Figure 17b). While the EPID beam profiles (Figure 17a) are well separated, the Starcheck beam profiles for varying bending current shunt voltage are overlapping at several off-axis distances. This could be the result of the fact that the EPID has a spatial resolution of 0.39 mm (distance between pixels), while the SC has a spatial resolution of 3 mm as a comparison.

Direct comparison between diode and EPID profiles is not advisable. It can, however, be concluded that deviations in beam quality following adjustments of bending current shunt voltage is readily detectable with the EPID without any additional build up. Using the beam profile, and the hump value, for evaluation of the beam quality measured with the EPID yield results comparable to those obtained with both the TPR measured with a scanning ionization chamber in the Blue Phantom water phantom as well as the Starcheck (SC with additional build-up) (Table 4).

The disadvantage one can discuss regarding the EPID is the lack of ability to measure a depth ionization curve. This third dimension, however, is as discussed above obtainable by evaluating the dose horns on the beam profile. The depth ionization curves measured with an ionization chamber (pre and post adjustment of bending current shunt voltage), normalized at dose maximum, reveals a shift of the dose maximum to a depth above that for the reference field (Figure 4d and Figure 4e). This indicates that the number of low-energy photons has increased when the bending current shunt voltage was decreased, which was also what was detected when seeing raised horns on the beam profile as measured with the EPID (Figure 4a).

3.2.2 Beam symmetry

All three measurement devices were capable of distinguishing an asymmetric profile from the reference (Figure 5). The profiles extracted from the EPID image obtained with a field size of 10 x 10 cm^2 (Figure 5b) indicate that using that kind of field for daily output monitoring will also allow beam symmetry to be observed at a daily basis if the smaller field size is used for linac output measurements. The bigger field size is, however, more preferable and therefore symmetry values are presented for a field size of 25 x 25 cm^2 for all three devices (Table 5).

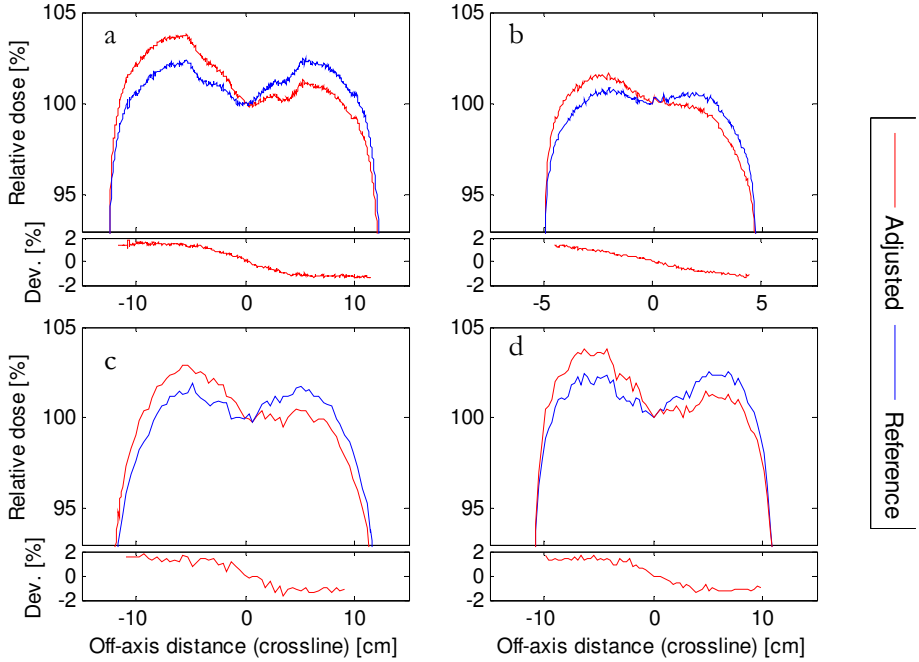

Figure 5. Symmetric reference profile and asymmetric profile after adjustment of steering current together with the deviation between the two profiles as a function of off-axis distance for a) EPID (25x25 cm^2), b) EPID (10x10 cm^2), c) diode in water phantom (25x25 cm^2) and d) Starcheck (25x25 cm^2).

Table 5. Effect of introduced known error in steering current on symmetry obtained with EPID, diode in water (DBP), Starcheck (SC) and the corresponding value of the T-sym parameter on the linac, for a field size of 25 x 25 cm^2.

Measurement device	EPID	DBP	SC	T-sym [V]
Before beam profile adjustment [%]	100.6	100.3	100.5	0.0
After beam profile adjustment [%]	103.3	103.0	103.0	-2.2
Change [%]	2.7	2.7	2.4	-

The greater resolution of the EPID, in comparison to DBP and SC is also noticeable (Figure 5). Profiles obtained with the diode were sampled with a sampling distance of 4 mm, while the distance between pixels in the EPID is approximately 0.4 mm. The standard deviation of the measurements at the reference conditions (before and after all adjustments) was ±0.2% (2SD) for the EPID symmetry values and ±0.1% (2SD) for the SC symmetry values, while the DBP value was the same at both occasions.

The results presented in this study will not give enough confidence in relating a symmetry change detected with the EPID to corresponding change in water. It can, however, be concluded that the EPID was able to detect a deviation on the transverse symmetry parameter from zero to approximately two (corresponding to the point at which an interlock will interrupt the machine). The limit recommended by the AAPM at which one should not conduct any treatment is however set at 1% (15). Therefore it would be desirable to measure at steering currents corresponding to smaller deviations in symmetry and increasing the number of values on the steering current for which measurements are carried out with these devices.

3.3 Daily quality control tests

3.3.1 Output

Evaluation of the absolute measurements carried out with ICW in the afternoons (Figure 6a), reveal that the linac used during this study has a drift in output. The deviation should also be seen when analysing the EPID (Figure 6b) and the linacheck (Figure 6d) afternoon and morning output measurements as well as the ICPMMA (Figure 6c) measurements performed in the afternoons.

Comparison between the EPID and LC measurements (calibrated against the ICW) carried out at the same occasions as the absolute measurements on the afternoons (Figure 6b and Figure 6c) indicates that there is better agreement between the EPID and ICW ($h=0$, $p=0.276$) than between the LC and the ICW ($h=1$, $p=0.009$). Comparison between the EPID and the ICPMMA ($h=1$, $p=1.3 \cdot 10^{-5}$) indicates that the data varies more for ICPMMA, thus being more uncertain than the EPID.

The drift in linac output was not as evident for the LC or the ICPMMA as for the other devices. Although ending up in deviations in the same magnitude as the other devices, the deviation detected by the LC does not increase continuously and does not demonstrate a trend as distinguishable as with the EPID and the ICW measurements.

Based on these results it can be stated that there is greater uncertainty with the LC system than with the EPID system. One explanation for the variation in the LC morning measurements is the uncertainty in positioning carried out by different RTTs each day. This uncertainty also applies for the ICPMMA measurements, where different physicists carry out the measurements every week. Note that the ICPMMA systematically measures a lower output than the EPID. The drift in output is apparent for both devices but the variance of the ICPMMA data is more prominent. Since the EPID has been proven to follow the trend detected by the ICW the interpretation of

this data is a need for calibration of the ICPMMA rather than the EPID. The fact that the EPID is mounted directly on the linear accelerator and has an automated positioning system eliminates the user dependence (not indicating that the uncertainty in the automated positioning is zero).

There was no great deviation detected between the measurements carried out with the EPID in the afternoons and the corresponding images acquired during the morning of the same day (Figure 6b). Even though a minor deviation was visible at a majority of the data points the mean deviation of the morning measurement from the corresponding afternoon measurement was only approximately -0.08% for the EPID (maximum deviation was -0.65%). This variation can be considered very low, taking into account the fact that the measurements most often are separated by approximately eight hours and that several conditions can change during these hours. Corresponding average deviation for the Linacheck was +0.19% (maximum deviation was +0.84%).

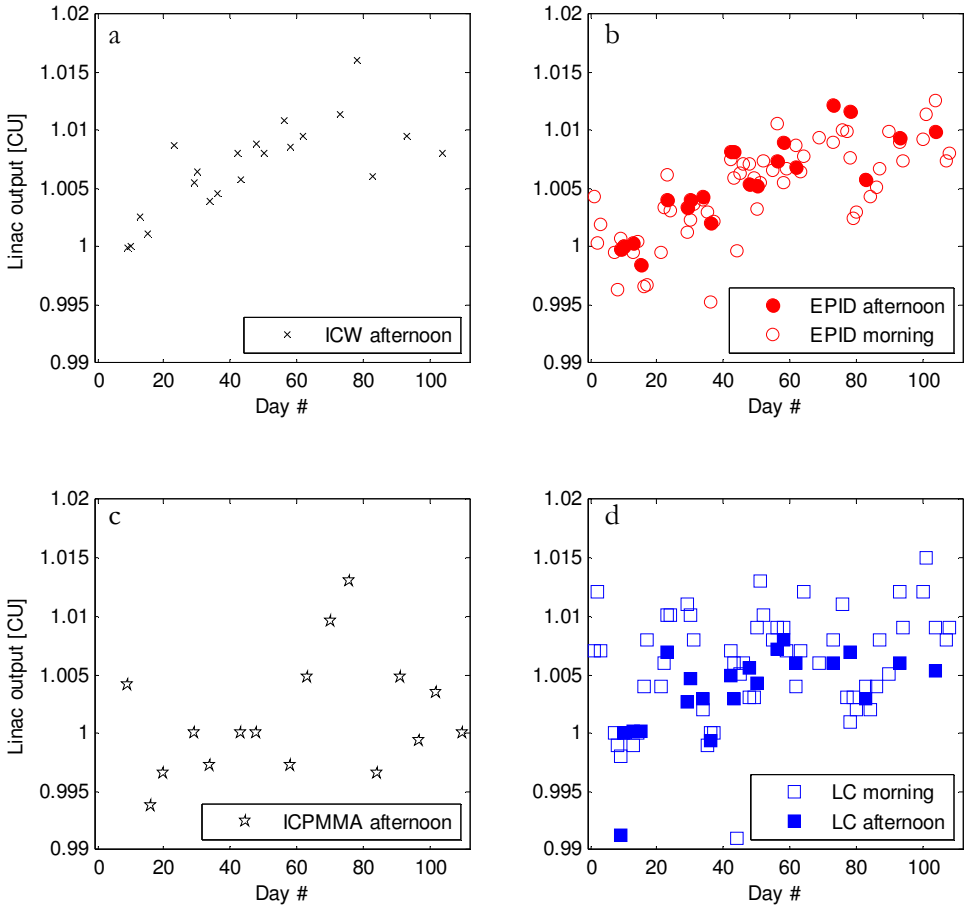

Figure 6. Output data for 6 MV collected with a) ionization chamber in water (ICW), b) EPID on a daily basis on mornings as well as in several afternoons, c) ionization chamber in PMMA (ICPMMA) and d) Linacheck (LC) on a daily basis as well as on several afternoons.

3.3.2 Field size dependence

Studying a plot of the linac output measured for both 10 x 10 cm^2 and 25 x 25 cm^2, together with a plot of the deviation between the output measured with the two different field sizes, indicates that the differences between the two field sizes are low (h=0, p=0.935) (Figure 7). It is evident that the drift in linac output and large deviations were detected regardless of used field size. Even

though the dosimetric calibration was carried out for a field size of 10x10 cm^2 the daily measurements with a field size of 25x25 cm^2 could be used. If correction is carried out, for the fact that the two different field sizes will render in different output values, it is clear that the deviation in output obtained for a field size of 25x25 cm^2 from the corresponding values for a field size of 10x10 cm^2 is negligible. For constancy control of the linac output one can therefore choose any of these field sizes, getting more advantage of the two-dimensional image for 25x25 cm^2.

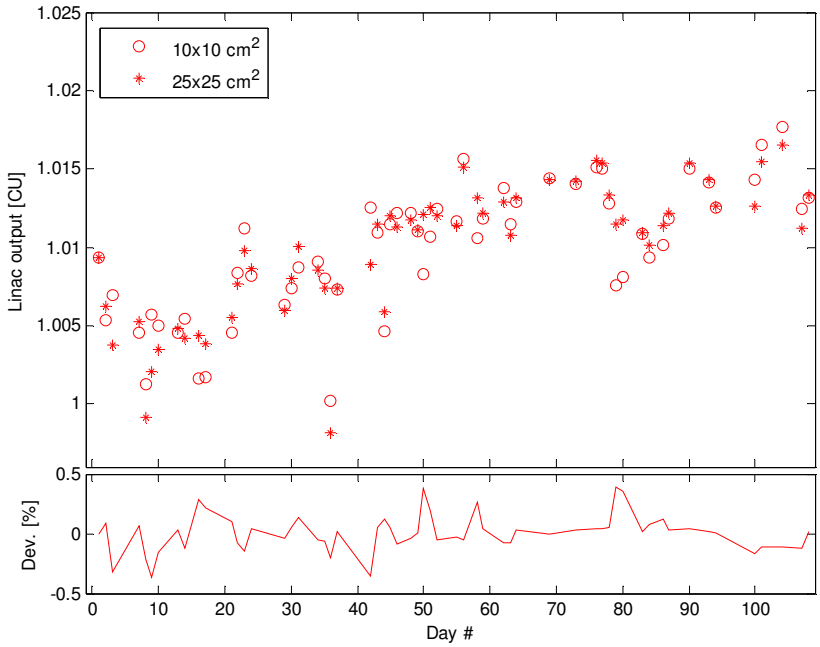

Figure 7. Comparison of EPID output measurements with a field size of 10x10 cm^2 and 25x25 cm^2 for 6 MV. The major plot is the linac output for the both field sizes (output factor corrected) and the subplot represents the deviation between the two at each measurement occasion.

3.3.2 SPC analysis of daily output control tests

The daily EPID measurements clearly indicate a drift in linac output (Figure 8) (also detected by the ICW measurements in the afternoons). The action limits obtained from SPC analysis would in the case of the EPID measurements indicate an action to be taken at or around day number 40 (Figure 8) and subsequent values after this day, lying outside the limits, also supported an action to be taken. No action was taken, since further evaluation of the correlation between the EPID and the ICW measurements as well as the LC measurements was desirable. In addition, the fixed limits were not exceeded by the LC values and the ICW measurements lay well within clinical limits.

In the case of the daily EPID measurements (Figure 8) the action limits obtained by SPC analysis and calculation of the standard deviation were not separated (both based on the 20 first data points). This could be an indication of a set of data consisting of only random variation. If the system would only consist of random variation, the EPID data would be an indication of that the EPID quality assurance system is a system that does not hold any systematic variation and that

the values found outside the limits with certainty were caused by the performance of the linear accelerator and not the quality assurance system.

Calculation of standard deviation and SPC analysis of the daily Linacheck measurements renders in a separation of the SPC and standard deviation limits (Figure 8). This could be an indication of a quality assurance system containing systematic variation. The fact is, however, that the number of data points used to obtain the limits is as few as 20 and the separation should only be taken as an indication of that the use of two standard deviations as action limits would be too insensitive.

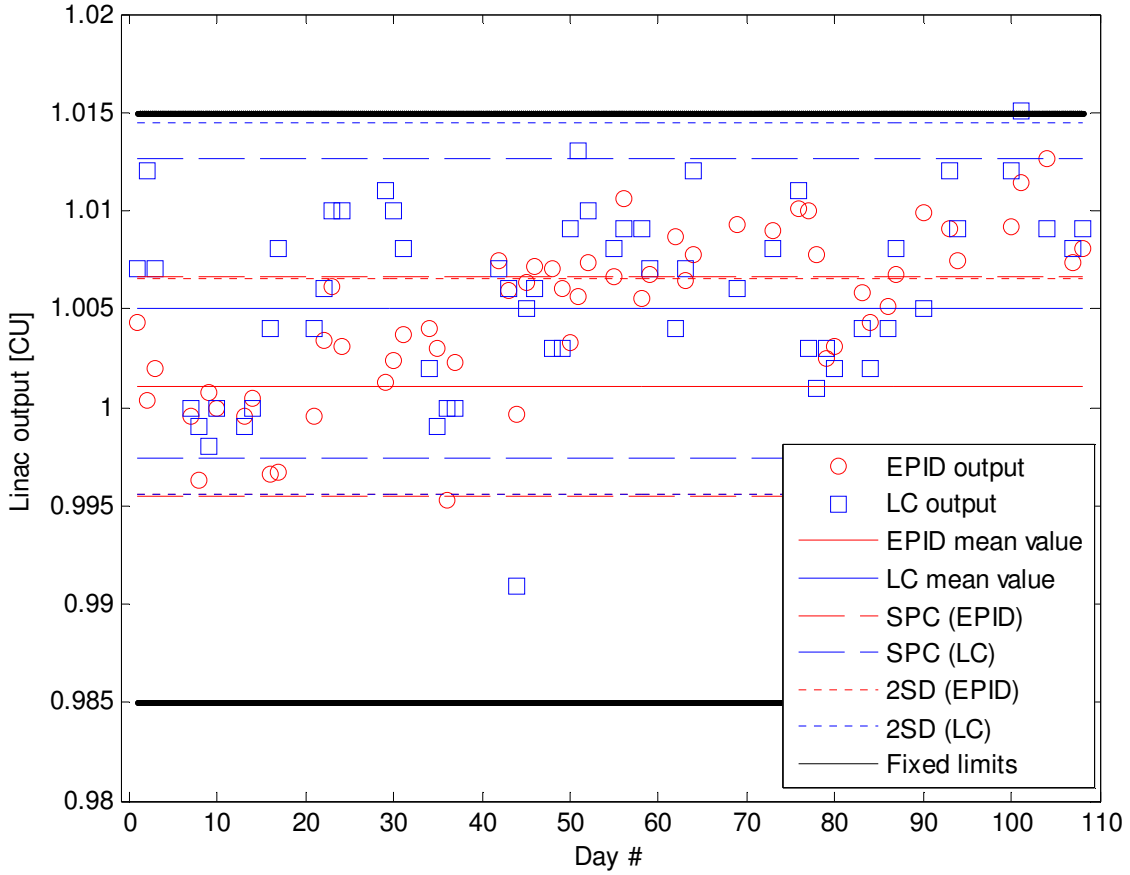

Figure 8. Output average chart for EPID and Linacheck daily measurements for 6 MV and a field size of 10x10 cm², presented together with limits obtained by applysing SPC analysis and calculation of the standard deviation of the first 20 data points. Fixed limit corresponds to the action limits set at a 1.5% deviation for the Linacheck.

Studying the daily Linacheck measurements (Figure 8) also reveals the fact that the drift in linear accelerator output as detected by the EPID and the ionization chamber (Figure 6) is not as clear for the Linacheck. Only a few points (one below the lower limit, two above the upper limit and one of those above the upper fixed limit) appear outside the SPC limits when using the Linacheck, which could be compared to 21 out of 58 data points lying above the upper SPC limit when the EPID was used. From these measurements it can be concluded that the Linacheck is less suitable as a device for daily output monitoring, based on the fact that there is more variation in the LC data than for the EPID. The interval defined by the upper and lower SPC limit is narrower for the EPID system than for the Linacheck (Figure 8), indicating more random variation

in the LC data. This fact can be attributed to several reasons, one being the inter-user/set-up variation and another being the fact that the Linacheck is an inexpensive measurement device. The conclusion is that this uncertainty would decrease if the daily output measurements were carried out using the EPID instead of the Linacheck.

One of the disadvantages of using the Linacheck is that the physicists have less time to act before the output reaches clinically unacceptable values in comparison to the EPID system (note that the fixed action level was reached for the Linacheck, but that only one data point lay outside the SPC limits before reaching that level). The EPID system, together with the SPC limits, will thus act as a more accurate system, with less disturbing variation and give more time to act before reaching clinically unacceptable deviations. This, in comparison to the Linacheck system and fixed limits at ±1.5%, for daily output monitoring.

The obtained range charts for the daily EPID and Linacheck measurements (Figure 9) indicates the same as the average charts, namely that the variation of the output values were greater for the Linacheck system. Noticeable is the fact that these range charts does not detect the continuous drift of the output. Instead they have only detected those data points deviating significantly from the day before, giving an indication of the uncertainty of the quality assurance system itself.

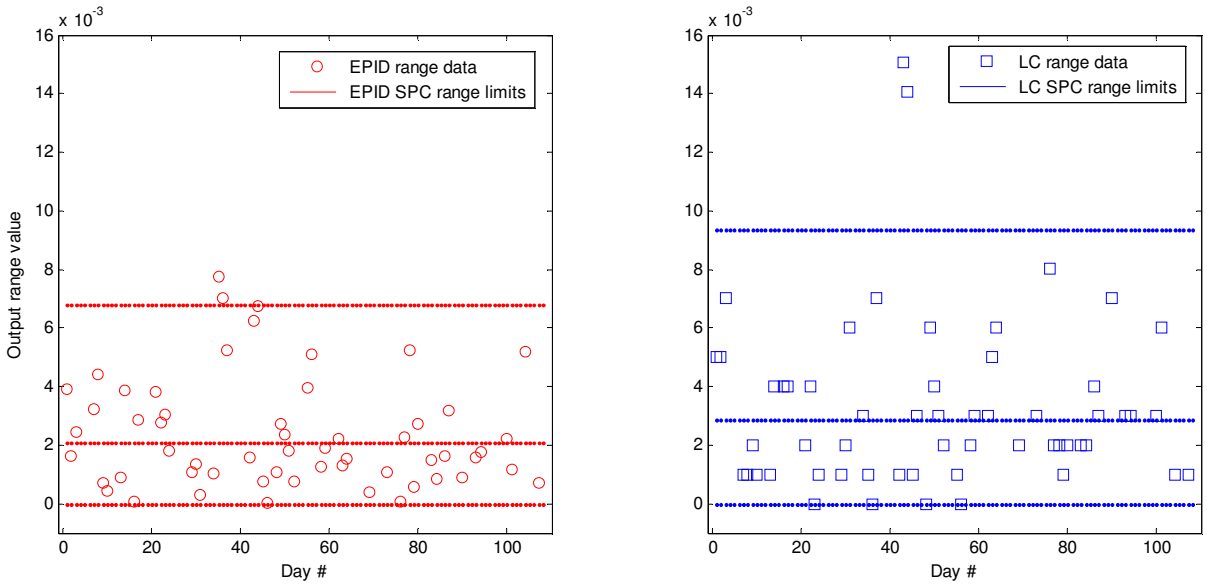

Figure 9. Output range chart for daily output measurements for 6 MV and a field size of 10x10 cm², carried out with a) EPID and b) Linacheck.

3.3.3 Beam quality and symmetry

When plotting all profiles extracted from the daily measurements with the EPID in one graph, together with the profiles corresponding to approximately ±0.3% change in $TPR_{20/10}$, it can be seen that they all lie within those two profiles (Figure 10). In this manner one can control how much the beam quality varies on a daily basis, giving an indication on how crucial it is to control the beam quality with for example an ionization chamber in a water phantom.

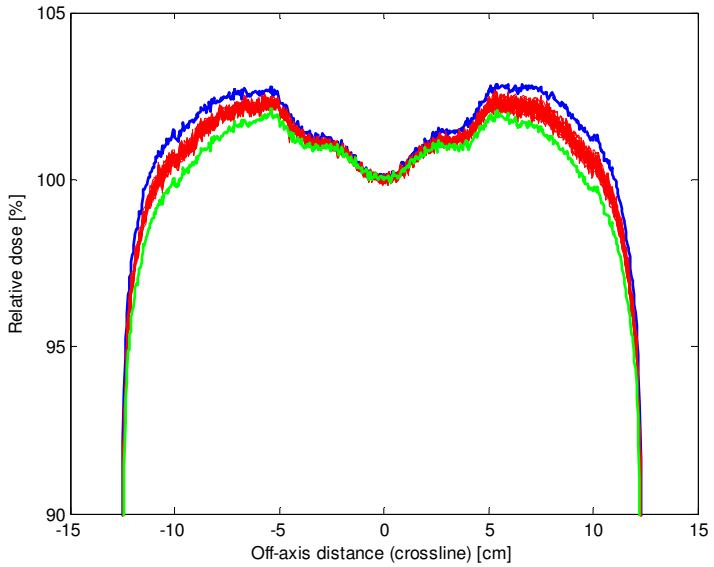

Figure 10. Beam profiles extracted from daily EPID measurements (red) together with beam profiles corresponding to a ±0.3% change in $TPR_{20/10}$ (blue and green).

3.3.4 SPC analysis of daily beam quality and symmetry control tests

The average chart of the hump values from the daily EPID measurements indicate a stability of the beam quality of the Varian linac used for this study (Figure 11a). The fact that two times the standard deviation will give limits lying inside the SPC limits is an indication of that utilizing the SPC analysis is a balance between the sensitivity and the resources available for further investigation and elimination of systematic variation. In this case the use of the standard deviation would be too sensitive and cause too much unnecessary workload.

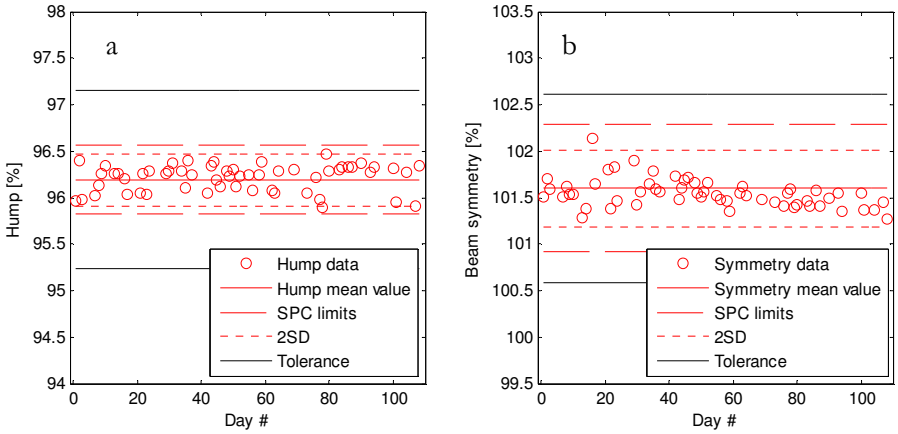

Figure 11. Average chart obtained from daily EPID measurements for 6 MV photons and a field size of 10x10 cm^2 for a) hump values and b) symmetry values. SPC limits and standard deviation based on the first 20 data points.

SPC analysis on the symmetry data collected on a daily basis with the EPID also indicates a stability of the linac regarding the beam profile (Figure 11b). As for the beam quality evaluation the standard deviation is too sensitive also in the case of the beam symmetry. Note that the tolerance levels were set at a ±1% deviation from the mean value, for both the beam symmetry and the

beam quality, as recommended by AAPM (15). In contrast to the daily EPID output values the beam quality as well as the beam symmetry can be concerned as so-called stable processes.

4 Conclusions

The study has proven that the EPID was suitable as a device for daily quality control of linac output, giving for example less variation in linac output than the Linacheck by the decrease in set-up uncertainty from the lesser user dependence of the EPID and the flexibility of the EPID as a two-dimensional detector. The two-dimensional images could in the same time be utilized for fast evaluation of the beam quality as well as the beam symmetry by extracting the beam profile. A correlation between TPR data, obtained by ionization chamber measurements in water, and hump values, obtained by extracting beam profiles from the acquired EPID images, was evident. Symmetry values obtained from the EPID images were also correlated with measurements in water. The fact that the EPID readout is fast and that the data is directly stored in a database is also one of its advantages. It has been proven that the EPID was able to detect drifts and deviations in the linac output. The response of the EPID has been proven to be similar to that for ionization chambers in water. Therefore, EPID measurements detecting a deviating output, lying outside the action levels, should lead to a correction of the linac output, by absolute measurement with an ionization chamber in water. Thereafter, the need for EPID calibration should be investigated.

Using statistical process control analysis for evaluation of daily measurements has proven to yield a good balance between sensitivity and resources available for corrective actions. The gap defined by the SPC limits has been proven to be useful for control of the need for improvements of the QA system or for comparison between two systems (as for the comparison between the daily EPID and LC output measurements). Utilizing SPC provides better knowledge on when to act on varying data points, in comparison to the use of for example fixed limits or to limits obtained by calculating the standard deviation based on a set of data points without any consideration to any time order. The standard deviation would be too sensitive in the case of the EPID hump and symmetry values, but too insensitive in the case of the LC output data. The SPC provide determination of the stability of the process. Hump and symmetry has, for example, been proven to be stable, whereas the detected drift in the linac output indicated an unstable process, by the SPC analysis.

5 Future prospects

With the positive results of this study the ambition is to implement the EPID as a quality assurance system at the department. With a total of eight accelerators, all similar to the one tested in this study (16), an implementation will also give the opportunity to gather further data for a future publication. Therefore the plan is also to extend the experiments regarding adjustments of beam quality as well as beam symmetry, giving a better relationship between the deviation detected by the EPID and the deviation this would have when measuring with either an ionization chamber or a diode in a 3D water phantom. The plan is to not only collect output, beam quality and beam symmetry data, but also to extend the study to evaluate the ability of the Varian aS1000 EPID to monitor the wedge. Furthermore, initial thoughts about controlling MLC function as well as controlling the time resolution in gated radiotherapy has been made.

It should also be mentioned that the EPID has only been utilized for quality assurance of the linac performance regarding the photon beam. The ambition was from the start to make use of the EPID also for QA of the electron beam as has been described for an iViewGT a-Si EPID (Elekta Oncology Systems, Crawley, UK) (17). After failed attempts to acquire images with an electron beam, Varian was contacted. It was confirmed that image acquisition does not function with electron beams. The explanation was the fact that the imager needs to be synchronised with the dose rate. The dose rate of the photon beam is synchronized with the use of a PLS (pulse length servo), while electron beam synchronization is carried out with a different technique. The conclusion is therefore that the hardware makes it impossible to acquire EPID images with electron beams and no further investigation regarding the suitability of the EPID as a QA device for electron beams was made.

Analysis of the acquired images during this study has been carried out off-line. The aim is to develop a graphical user interface (GUI) for fast evaluation of the acquired images. The process of developing a GUI has been started by the author of this report and will continue during the implementation of the EPID as a quality assurance device. This development will be in close collaboration with the physicists and radiotherapy technologists (RTT) at the department. A first version of the GUI, not yet ready for clinical use, has been developed to give a quick indication of the accelerator performance, giving a value of the output and a green or a red signal indicating whether or not any action is necessary. Figure 12a illustrate the first view of the GUI where it is possible to select the beam quality as well as the field size of interest and get statistics on output, beam quality and symmetry. The result of pressing the calculate button is presented in Figure 12b. In the case presented here the most resent output value lies outside the SPC limits. Therefore a red box appears, recommending the one that has carried out the test to contact the physicist in charge of quality assurance of the accelerators. Beam quality and symmetry, on the other hand, lies within the action limits, therefore presenting those values in a green box. In this version of the software an average chart and a range chart of the output values is also presented. These plots are perhaps not of interest for the treatment personnel, but for a physicist they are, together with for example the beam profile, of interest. The physicist, treatment personnel and also technicians will therefore work together to improve and adopt the GUI with the different needs in mind.

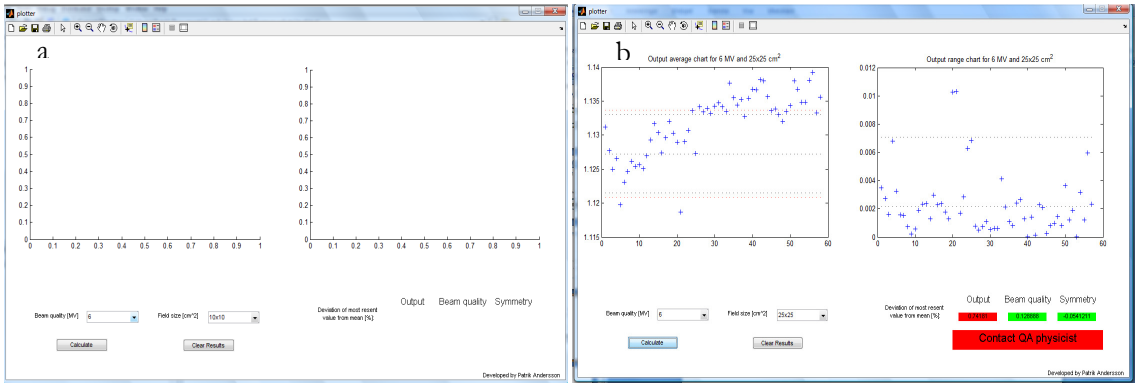

Figure 12. First version of graphical user interface for fast evaluation of acquired EPID images. The figure illustrate a) the view where beam quality and field size for evaluation is to be selected and b) where the deviation of output, beam quality and symmetry from the reference is is presented after pressing the buttom "Calculate".

6 References

1. **Ringborg U, et al.** The Swedish Council on technology Assessment in Health Care (SBU) Systematic Overview of Radiotherapy for Cancer including a Prospective Survey of Radiotherapy Practice in sweden 2001 - Summary and Conclusion. *Acta Oncologica.* 2003, Vol. 42, 5/6.

2. **Mijnheer B, Battermann J, Wambersie A.** What degree of accuracy is required and can be achieved in photon and neutron therapy. *Radiother. Oncol.* 1987, Vol. 8.

3. **SSM.** SSMFS 2008:33 Strålsäkerhetsmyndighetens föreskrifter om medicinsk strålbehandling. *Strålsäkerhetsmyndigheten*, 2008.

4. **AAPM.** Task Group 40 report: Comprehensive QA for radiation oncology. *American Association of Physicists in Medicine*, 1994.

5. **Ahnesjö A, Aspradakis MM.** Dose calculations for external photon beams in radiotherapy. *Phys. Med. Biol.* 1999, Vol. 44.

6. **Curtin-Savard A, Podgorsak E B.** An electronic portal imaging device as a physics tool. *Medical Dosimetry.* 1997, Vol. 22, 2.

7. **Kirby M C, Williams P C.** the use of an electronic portal imaging device for exit dosimetry and quality control measurements. *Int. J. Radiation Oncology Biol. Phys.* 1995, Vol. 31, 3.

8. **Budgell G J, Zhang R and Mackay R I.** Daily monitoring of linear accelerator beam parameters using an amorphous silicon EPID. *Phys. Med. Biol.* 2007, Vol. 52.

9. **van Elmpt W, McDermott L, Nijsten S, Wendling S, Lambin P, Mijnheer B.** A literature review of electronic portal imaging for radiotherapy dosimetry. *Radiotherapy and Oncology.* 2008, Vol. 88, 3.

10. **Pawlicki T, Whitaker M, Boyer AL.** Statistical process control for radiotherapy quality assurance. *Med. Phys.* 2005, Vol. 32, 9.

11. **McDermott L N, Nijsten S M J J G, Sonke J-J, Partridge M, v Herk M, Mijnheer B J.** Comparison of ghosting effects for three commercial a-Si EPIDs. *Med. Phys.* 2006, Vol. 33, 7.

12. **McDermott L N, Louwe R J W, Sonke J-J, van Herk M B, Mijnheer B J.** Dose-response and ghosting effects of an amorphous silicon electronic portal imaging device. *Med. Phys.* 2004, Vol. 31, 2.

13. **IAEA.** TRS-398 - Absorbed Dose Determination In External Beam Radiotherapy. Vienna : *International Atomic Energy Agency*, 2000.

14. **IEC.** Medical electron accelerators in the range 1 MeV to 50 MeV - Guidlines for functional performance characteristics (IEC publication 977). Geneva : *International Electrotechnical Commission*, 1989.

15. **AAPM.** Task Group 142 report: Quality assurance of medical accelerators. *American Association of Physicists in Medicine*, 2009.

16. **Sjöström D, Bjelkengren U, Ottoson W, Behrens C F.** A beam-matching concept for medical linear accelerators. *Acta Oncologica.* 2009, Vol. 48, 2.

17. **Beck J A, Budgell G J.** Electron beam quality control using an amorphous silicon EPID. *Med. Phys.* 2009, Vol. 36, 5.

18. **ICRU.** Prescribing, reporting and recording photon beam therapy (report 62). *International Commission on Radiation Units and measurements.* 1999.

19. **Podgorsak E B.** Radiation oncology physics: A handbook for teachers and students. *International Atomic Energy Agency*, 2005.

20. **IPEM.** Physics aspects of quality control in radiotherapy. *The Institute of Physics and Engineering in Medicine*, 1999.
21. **Antonuk, L E.** Electronic portal imaging devices: a review and historical perspective of contemporary technologies and research. *Phys. Med. Biol.* 2002, Vol. 47.
22. **Louwe R J W, et al.** The long-term stability of amorphous silicon flat panel imaging devices for dosimetry purposes. *Med. Phys.* 2004, Vol. 31, 11.
23. **Van Esch A, Depuydt T, Huyskens D P.** the use of an aSi-based EPID for routine absolute dosimetric pre-treatment verfification of dynamic IMRT fields. *Radiotherapy and Oncology.* 2004, Vol. 71.
24. **Vieira S C, Bolt R A, Dirkx M L P, Visser A G, Heijmen B J M.** Fast, daily linac verification for segmented IMRT using electronic portal imaging. *Radiotherapy and Oncology.* 2006, Vol. 80, 1.
25. **Mamalui-Hunter M, Li H, Lowa D A.** MLC quality assurance using EPID: A fitting technique with subpixel precision. *Med. Phys.* 2008, Vol. 35, 6.
26. **Baker S J K, Budgell G J, MacKay R I.** Use of an amorphous silicon electronic portal imaging device for multileaf collimator quality control and calibration. *Physics in Medicine and Biology.* 2005, Vol. 50, 7.
27. **Chang J, Obcemea C H, Sillanpaa J, Mechalakos J, Burman C.** Use of EPID for leaf position accuracy QA of dynamic multi-leaf collimator (DMLC) treatment. *Medical Physics.* 2004, Vol. 31, 7.
28. **Samant S, Jain J, Sobczak D, Crawford B, Coffey D, Xia J.** EPID based quality assurance for collimation verification in external beam radiotherapy. *Medical Physics.* 2003, Vol. 30, 6.
29. **Yang Y, Xing L.** Quantitative measurements of MLC leaf displacement using an electronic portal imaging device. 2004, Vol. 49, 8.
30. **Wheeler D J, Chambers D S.** Understanding statistical process control. *SPC Press,* 1992.
31. **Breen SL, Mosely DJ, Zhang B, Sharpe MB.** Statistical process control for IMRT dosimetric verification. *Med. Phys.* 2008, Vol. 35, 10.
32. **Pawlicki T, Mundt AJ.** Quality in radiation oncology. *Med. Phys.* 2007, Vol. 34, 5.
33. **Gérard K, et al.** A comprehensive analysis of the IMRT dose delivery process using statistical process control (SPC). *Med. Phys.* 2009, Vol. 36, 4.
34. **Pawlicki T, Whitaker M.** Variation and control of process behaviour. *Int. J. Radiation Oncology Biol. Phys.* 2008, Vol. 71, 1.
35. **Thor J, Lundberg J, Ask J, Olsson J, Carli C, Pukk Härenstam K, Brommels M.** Application of statistical process control in healthcare improvement: systematic review. *Qual Saf Health care.* 2007, Vol. 16.

Appendix I - General quality assurance of medical linear accelerators

In order to meet the International Commission on Radiation Units and Measurements (18) recommendation that the dose delivered to the patient is within ±5% (2 SD) of the prescribed dose, there are a lot of requirements on the many steps involved in delivering dose to a target volume. The performance of linear accelerators is certainly a very important part and must therefore be thoroughly tested. Recommendations for general quality assurance tests for medical linear accelerators can be found in the American Association for Physics in Medicine (AAPM) Task Group (TG) 142 report (15). The TG-142 report is an update of the AAPM TG-40 report (4) and also includes recommendations for newer techniques, such as asymmetric jaws and multi-leaf collimation (MLC). The parameters to be tested are divided into different categories; dosimetry, mechanical, safety and respiratory gating. Also, each parameter is recommended to be tested with a certain frequency (daily, weekly, monthly or annually). The purpose of the tests is to ensure that the parameters do not differ significantly from the baseline data that has been acquired, most often, during the commissioning of the accelerator. If deviations are obtained they should not exceed the action levels. Deviations exceeding the action levels should render in a corrective action, assuring that the deviation will not exceed the existing tolerance level. The tolerance levels are set to meet the recommendation so the dose delivered to the patient will be within ±5% (2 SD). That means that the quality assurance and the tolerance levels make sure that the overall dosimetric uncertainty is no more than the order of ±5% (2 SD). Also the overall spatial uncertainty is recommended to be within ±5% (2 SD). It should be noted that these uncertainties of 5% (2 SD) represent a 95% confidence level. The 5% tolerance level is common and other recommendations support this level. For example Ahnesjö (5) et al. imply have concluded, by identifying the errors in the dose delivery chain, that dose calculations does not need to be better than 2% with a tolerance level at 3.1% (1 SD). This implies, also, an uncertainty of 1% in determining the absorbed dose at the calibration point.

The TCP and NTCP curves represent the change in response expected for a given change in delivered dose. An increase in uncertainty therefore, potentially, worsens the clinical outcome as it might imply either a reduction in the TCP or an increase in the NTCP (19). The clinical requirements on accuracy are therefore based on very sensitive tumours and normal tissues.

A requirement for further decrease in the uncertainty in radiotherapy is quality assurance. Quality assurance is namely an important part in reducing uncertainties and errors in dosimetry, treatment delivery, treatment planning, equipment performance etc. Quality assurance also reduces the likelihood of accidents and increases the possibility to identify and resolve them if the do take place (19). Ultimately, the objective of quality assurance is to improve the patient safety and guarantee that the complications on the normal tissue are kept as low as reasonably achievable (ALARA).

Several recommendations on how to ensure that a quality assurance program meets the demands on accuracy and patient safety in radiotherapy have been published (15; 20). For a medical linear

accelerator they in general all include demands on initial specification of equipment and the equipment operation, service etc., as required by the user. Further the general quality assurance program also include acceptance testing, commissioning for clinical use and quality control tests. The acceptance testing and commissioning, together, will set up the baseline values of performance to which all future quality control tests will be referred. The quality control tests ensure that the performance of the linear accelerator lies within accepted tolerances obtained from the baseline values. If values from quality control tests lies outside the tolerance level actions are to be made. For a quality assurance program to function it is therefore necessary to specify action levels and which actions that are required if these limits are exceeded. Since the baseline values are referred to when carrying out a quality control test, it is also necessary to specify the parameters to be tested, at which frequency they are to be tested, the geometry of the test and also the specific equipment to be used to undertake the test. Recommended QA devices and equipment often include ionization chambers, water scanning phantoms, diodes and flat-panel multi-detector arrays. The possibility, however, to use amorphous silicon electronic portal imaging devices is not as well documented and is the subject of investigation in this study.

Appendix II – Amorphous silicon electronic portal imaging devices

Electronic portal imaging devices were primarily developed for geometric verification of patient set-up and have later expanded its use into dose verification, either by pre-treatment or *in-vivo* measurements. Therefore it has replaced film measurements which have been seen as the golden standard in geometric verification of patient set-up for a long time. Perhaps the biggest advantage of using EPID instead of film measurements is the fact that the EPID is mounted directly on the linear accelerator (Figure 1) and that it enables multiple acquisitions in a short amount of time.

Many different technologies have existed during the development of EPIDs and Antonuk (21) has delivered an extensive review of these different techniques. Only three of these techniques have proven to yield adequate, clinically useful, information and those are camera-mirror-lens based systems, the scanning liquid filled ionization chamber design and active matrix flat-panel imagers. Since only the latter of these techniques has been utilized in this study it will be the only technique described in this context.

Indirect detection active matrix, flat-panel EPIDs became commercially available for the first time in the year 2000 (21). This was the year the Portal Vision aS500 EPID was introduced by Varian Medical Systems EPID, from which the EPID utilized in this study, the Portal Vision aS1000 (Varian, Inc., Palo Alto, CA, USA), evolved from (same active area and acquisition software, higher resolution; 1024x768 pixels (11)). The detector is based on a discrete photo sensor of hydrogenated amorphous silicon (a-Si) photodiode located in each pixel (21). The photo sensor is overlaid with an x-ray converter which consists of a metal plate and a scintillator. The x-ray converter simply converts the incident x-ray energy into light. The light emitted by the scintillator, position directly above the photo sensor, is converted to electron-hole pairs when entering the photo sensor (Figure 13). In the case of the Portal Vision aS1000 EPID the scintillator is a phosphor screen with a thickness of approximately 0.4 mm. The created charge is stored in the capacitive element in each pixel until readout.

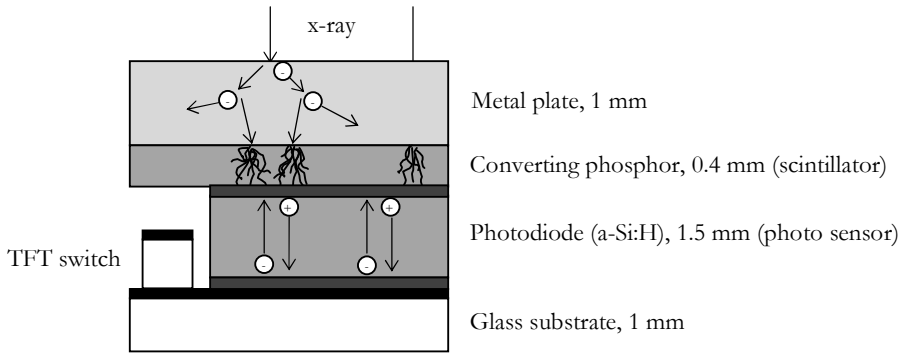

Figure 13. Schematic figure of the components of an amorphous silicon electronic portal imaging device.

In addition to above mentioned components the a-Si EPID consist of an electronic acquisition system, for operation of the array, extraction and processing of the analogue signal, as well as a host computer for processing, display and storage of digital images. The combination of these components render, in the case of the aS1000, in an active area of 40x30 cm^2. With a resolution of 1024x768 pixels the spatial resolution is approximately 0.0391 cm. Furthermore acquisition can be carried out at a maximum frame rate of 9.574 frames per second at energies between 4 MV and 25 MV and a dose rate between 50 and 600 MU per minute.

As well as previous mentioned advantages of the a-Si EPID it should be pointed out that the compact a-Si EPID enables real time, digital readout with the possibility of both radiographic and fluoroscopic readout. Furthermore, in comparison to other EPID techniques, the a-Si EPID has a highly linear signal response and can be utilized for dosimetric purposes. It is also more resistant to radiation damage, which of course is of high importance if it is to be used as a tool for routine quality assurance (21). The electronics at the periphery of the matrix must be paid attention to, since they are more sensitive to radiation damage than the active area itself. Most importantly the a-Si EPIDs have an advantage in the high image quality.

The suitability of a-Si EPIDs for dosimetry purposes has previously been investigated (22) and the many advantages of the a-Si EPID has rendered in increased implementation of the imager in for example dose verification in intensity modulated radiotherapy (IMRT) (23; 24). Implementation in quality assurance of the linear accelerator has not progressed as quickly, and even though further investigation is needed some studies have proven its suitability as a quality assurance tool (8).

At the department where this study has been undertaken the use of EPID has to some extent been implemented with a focus on quality assurance of multi-leaf collimator (MLC) performance. The positioning of the MLC leafs as the gantry rotates is for example checked with a so-called Picket Fence Test. An image of the MLC position is compared to a reference image where some known deviations are introduced (0.5 mm displacement error, 0.5 mm and 1.0 mm widening of the field defined by the MLC). The use of EPIDs for MLC quality assurance has also been thoroughly investigated in the literature (25; 26; 27; 28; 29). Furthermore a test to ensure that the linac is able to deliver specified number of monitor units with varying MLC speed is carried out. The EPID is also used to ensure that the linac is able to vary the gantry speed as well as to vary the dose rate. The tests carried out with the EPID at the department are evaluated in Portal Dosimetry (Varian Inc., Palo Alto, CA, USA), where the images are compared to reference images.

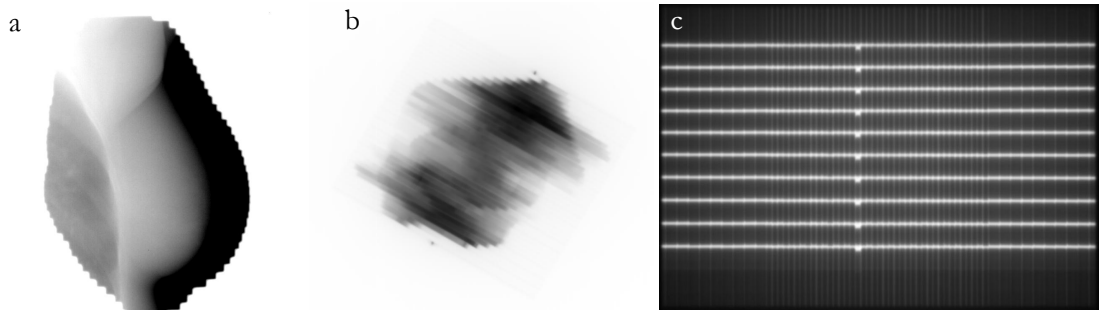

Figure 14. Example of a) geometric verification of patient position, b) integrated of rapid arc plan and c) fence test for control of MLC (courtesy of Ulf Bjelkengren).

Appendix III – Statistical process control

The mathematical formulation behind statistical process control (SPC) has been described in the literature (30) and its suitability as a statistical tool in radiotherapy has in some extent been investigated (10; 31; 32; 33). This appendix will serve as a summary of the most fundamental terminology and equations and its application to quality assurance in radiotherapy.

Quality control of medical linear accelerators is often carried out by comparing a measurement of some parameter with a given specification or baseline (34). Deviations are then investigated as they occur rather than studying the process, searching for eventual problems and solving them before it becomes critical (32). Quality assurance processes consists of random as well as systematic errors. The use of mean value and standard deviation for evaluation of the data or the use of fixed action limits is currently the most common approaches and does not adequately distinguish the one from the other. Detection as well as reduction of systematic errors is therefore not possible. The main purpose of using SPC in radiotherapy is to be able to identify and deal with the systematic errors by introducing action levels that are able to separate random from systematic errors (10). The SPC concept has in some extent been adopted in healthcare (35). In radiotherapy it has for example been utilized for verification of IMRT dose delivery and has the potential to serve as a good tool for quality assurance of medical linear accelerators (31; 33).

In 2005, Pawlicki et al. (10) published a summarized version of the detailed presentation of the mathematical formalism of SPC by Wheeler and Chambers (30). The summarized description of the formalism given here has been adopted and revised for an implementation in routine quality assurance of medical linear accelerators with an a-Si EPID.

Quality assurance of medical linear accelerators is measuring relevant parameters and acquiring a set of numerical data $x_1, x_2, x_3, \ldots x_N$, where N is the number of measurements. Assume that the data can be described by a normal distribution with mean $\mu(x)$ and standard deviation $\sigma(x)$. To obtain so-called process control charts, subgroup averages, $\bar{x}$, and subgroup ranges, R, are calculated according to equation 3 and 4, respectively, where n is the subgroup size and m the number of subgroups (10).

$$\bar{x}_{j=1,\ldots,m} = \left((1/n)\sum_{i=1}^{n} x_i\right)_j \quad \text{(Eq. 3)}$$

$$R_{j=1,\ldots,m} = \left(\max(x_1, x_2, x_3, \ldots x_n) - \min(x_1, x_2, x_3, \ldots x_n)\right)_j \quad \text{(Eq. 4)}$$

Subgroup averages, $\bar{x}$, can according to the central limit theorem also be described as a normal distribution with mean $\mu(\bar{x})$ and standard deviation $\sigma(\bar{x})$, which can be related to the parent distribution according to equation 5 and 6, respectively (10).

$$\mu(\bar{x}) = \mu(x) = \bar{\bar{x}} \quad \text{(Eq. 5)}$$

$$\sigma(\bar{x}) = \sigma(x)/\sqrt{m} \quad \text{(Eq. 6)}$$

The mean and standard deviation of subgroup ranges can also be related to the parent distribution, in accordance with equation 7 and 8, respectively (10).

$$\mu(R) = d_2 \cdot \sigma(x) = \frac{1}{m}\sum_{i=1}^{m} R_i = \overline{R} \qquad \text{(Eq. 7)}$$

$$\sigma(R) = d_3 \cdot \sigma(x) \qquad \text{(Eq. 8)}$$

The d_2 and d_3 factors are the so-called bias correction factors and depend upon the subgroup size, *n*, as well as the underlying distribution of the data. It has, however, been empirically proven that the dependence on assumed distribution is not that strong, even though the calculated values of the bias correction factors used in this study is obtained with the assumption that the underlying distribution is normal (10). Equation 7 and a combination of equation 6 with equation 7 and equation 7 with equation 8 render in equations 9, 10 and 11, respectively (10).

$$\sigma(x) = \frac{\mu(R)}{d_2} \qquad \text{(Eq. 9)}$$

$$\sigma(\bar{x}) = \frac{\mu(R)}{\left(d_2 \cdot \sqrt{m}\right)} \qquad \text{(Eq. 10)}$$

$$\sigma(R) = \frac{d_3}{d_2} \cdot \mu(R) \qquad \text{(Eq. 11)}$$

These three equations describe the variation in the theoretical distribution of the measured data. The mean of the subgroup averages and the mean of the subgroup ranges can be estimated as the arithmetic averages of the subgroup averages and ranges respectively (10). $A_c = \overline{\overline{x}}$ and $R_c = \overline{R}$ will then serve as the centreline in the two process behaviour charts (average and range charts). The action thresholds are set by the upper and lower limits calculated according to equations 12 and 13 for the average chart and equations 14 and 15 for the range chart, respectively (10).

$$A_u = \overline{\overline{x}} + t \cdot \frac{\overline{R}}{\left(d_2 \cdot \sqrt{n}\right)} \qquad \text{(Eq. 12)}$$

$$A_l = \overline{\overline{x}} - t \cdot \frac{\overline{R}}{\left(d_2 \cdot \sqrt{n}\right)} \qquad \text{(Eq. 13)}$$

$$R_u = \overline{R} \cdot \left(1 + t \cdot \frac{d_3}{d_2}\right) \qquad \text{(Eq. 14)}$$

$$R_l = \overline{R} \cdot \left(1 - t \cdot \frac{d_3}{d_2}\right) \qquad \text{(Eq. 15)}$$

The parameter *t* is a scaling factor for the limits and has empirically been set to a value of 3 (10). The value was proven to give a good balance between the sensitivity of the charts and the re-

sources available to investigate systematic errors (10). It should be noted that the limits calculated in this manner only assumes local homogeneity within the subgroups and not a global homogeneity for the whole data set as the use of single dispersion statistics does. Acquiring successive subgroups will therefore in the case of SPC make it possible to detect systematic errors in the process against the background noise (10). The advantages of the SPC concept in comparison to single dispersion statistic is therefore the fact that it is easier to ensure subgroup homogeneity than homogeneity over an entire data set, as well as the fact that the sensitivity in detecting overall changes in the process behaviour is much greater with SPC.

In the case of daily quality assurance, as is investigated in this study, data comes along fairly slowly with measurements once every day. The measurement on each and every single day will in this situation be a subgroup on its own. For a subgroup of one data point the upper and lower limits can be calculated using d_2 and d_3 for a subgroup of n=2 (Table 6). Note that values on d_2 and d_3 is only to be used in combination with equations stated in this text since a different set of bias correction factors are to be used together with other dispersion statistics than the normal distribution as is used in this study (10). With only one data point each subgroup will automatically be homogenous, but it will require a so-called moving range. A moving range is defined as the difference between two successive measurements from two successive dates.

The optimal subgroup size is one where the data points in it are homogeneous. Choosing a larger homogenous subgroup would be preferred, but a large subgroup with inhomogeneous data decreases the usefulness of the system (10). One must therefore be certain of the homogeneity of the subgroup before making any decisions on eliminating eventual systematic errors based on the data collected. Another issue is the number of subgroups to be used for calculation of the limits. It can be stated that the number of subgroups should be statistically significant. When starting to evaluate a process by applying SPC one could be confident in calculating process behavior limits relatively early. Before ending up with a statistically significant number of subgroups (approximately between 20 and 30 (10) data points within the limits will be an evidence of a stable process with only random errors. At the same time data point outside the limits should be seen as systematic errors and should be further investigated. In the case of this study the EPID measurements are compared to measurements with the Linacheck (routinely used as daily QA tool) collected at the same occasions as the EPID data, and therefore directly gives an indication if a measurement is object to a systematic error.

The use of SPC and process behavior charts should be continued by comparing averages and ranges to the obtained limits. As mentioned, continued daily measurements within the process behavior limits is a proof of the process being stable (Figure 15a) (10). Readings outside the limits should on the other hand be an indication of an unstable process and actions to identify and remove systematic errors should be taken (Figure 15b) (10). To secure a stable process daily measurements should be continued after elimination of the systematic error and if the values then continues to be within the process behavior limits the systematic error could be considered eliminated and the process stable. One should emphasize the fact that limits acquired from SPC analysis should not replace the clinical requirements on a treatment delivery system. A data point outside the clinical requirements, even if within the limits set by the control charts, should always render in further investigation. Further investigation should also be made if a data point, inside or

outside clinical requirements, lies outside the action thresholds of the control chart (SPC limits outside the clinical limits would, however, indicate an inadequate quality assurance system). The only state where one could be sure that the process is stable is in the case of repeated data points within both clinical requirements and action thresholds set by the control charts (Figure 15a).

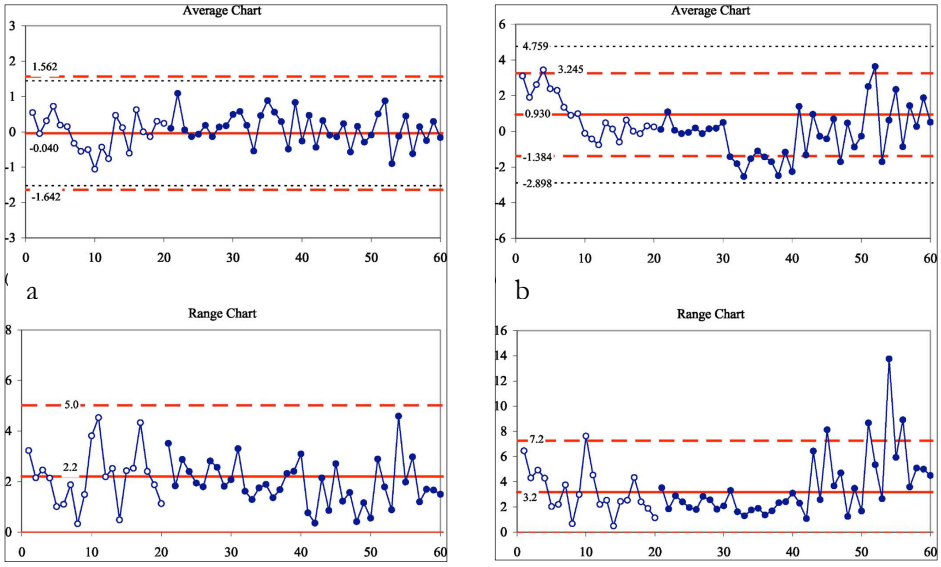

Figure 15. Average and range charts for a) a process with only random variation and b) a process containing random and systematic variation (Adopted from Pawlicki et al. (10)).

Table 6. Bias correction factors, d_2 and d_3, for different subgroup sizes, *n*.

n	d_2	d_3
2	1.128	0.8525
3	1.693	0.8884
4	2.059	0.8798
5	2.326	0.8641
6	2.534	0.8480
7	2.704	0.8332
8	2.847	0.8198
9	2.970	0.8078
10	3.078	0.7971
11	3.173	0.7873
12	3.258	0.7785
13	3.336	0.7704
14	3.407	0.7630
15	3.472	0.7562
20	3.735	0.7287
25	3.931	0.7084
30	4.086	0.6927
40	4.322	0.6692
50	4.498	0.6521
100	5.015	0.6052

Appendix IV – Figures and tables

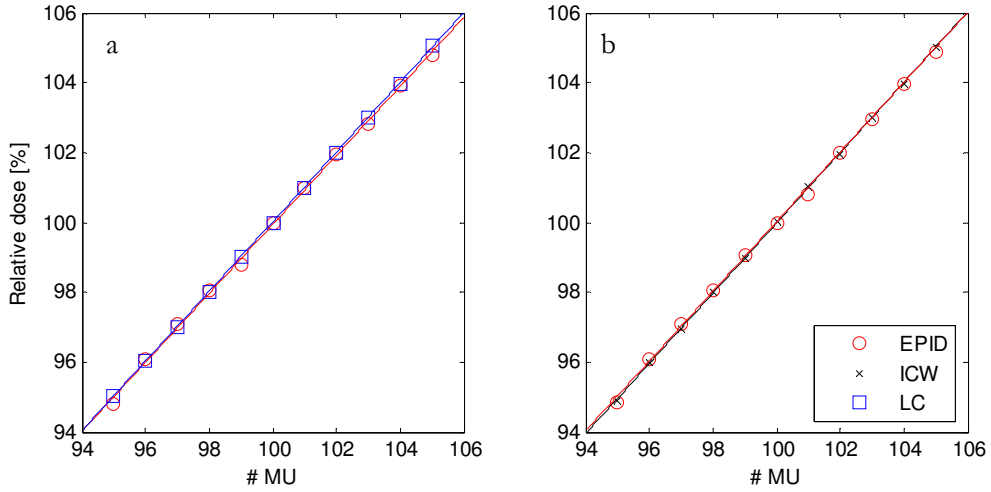

Figure 16. Comparison of the response as a function of specified number of MU between a) EPID and Linacheck and between b) EPID and ionization chamber in water for 15 MV photons.

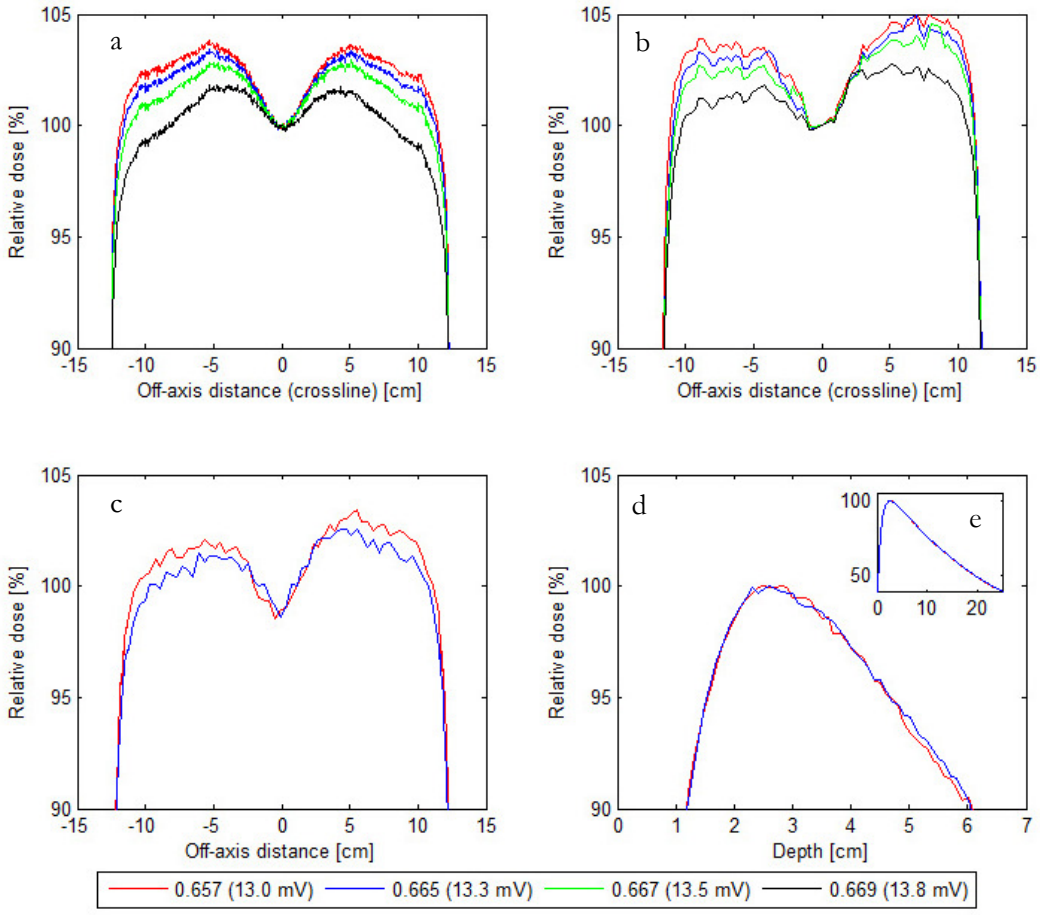

Figure 17. Results of measurements for 15 MV after adjustment of the bending current shunt voltage to obtain varying beam quality. The varying beam quality is presented here as four different beam profiles acquired with a) the EPID and b) the Starcheck, as well as c) profiles acquired with a diode and the Blue Phantom for the reference beam quality and the lowest beanding current and d) depth ionization curves measured with an ionization chamber in Blue Phantom for the same two beam qualities as measured with the diode (e) the two entire depth ionization curves).

Table 7. Values of TPR20/10 and hump, together with the corresponding deviation from the reference value, obtained with ionization chamber in water (brand), EPID and Starcheck for four different values on the bending current shunt voltage for 15 MV photons.

Bending	ICW		EPID		Starcheck	
current [mV]	$TPR_{20/10}$	Dev.[%]	Hump(±2SD)[%]	Dev.[%]	Hump(±2SD) [%]	Dev.[%]
33.0	0.758	-0.26	97,48(±0.06)	0,38	98.53(±0.10)	-0.55
33.5	0.759	-0.13	97,31(±0.06)	0,21	99.29(±0.10)	0.21
34.0	0.760	0	97,11(±0.06)	0	99.08(±0.10)	0
35.5	0.763	0.39	96,19(±0.06)	-0,94	97.49(±0.10)	-1.61

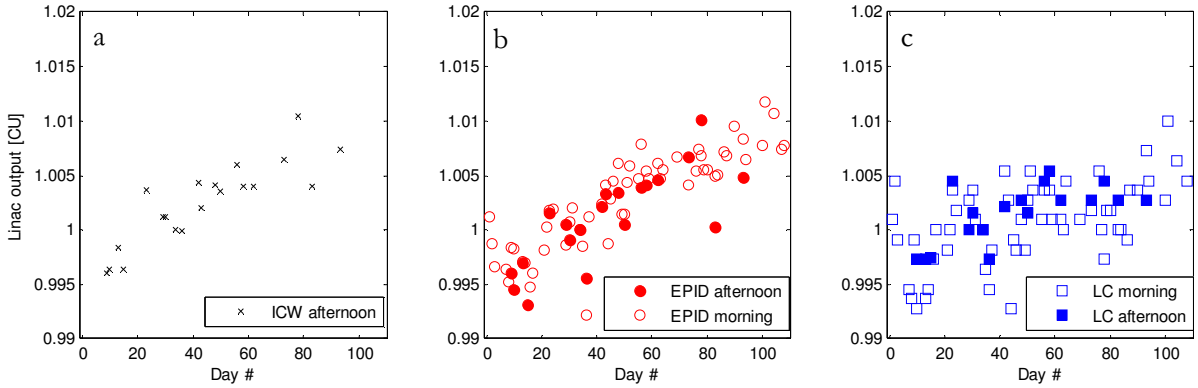

Figure 18. Output data for 15 MV collected with a) ionization chamber in water (ICW), b) EPID on a daily basis on mornings as well as in several afternoons and c) Linacheck (LC) on a daily basis as well as on several afternoons.

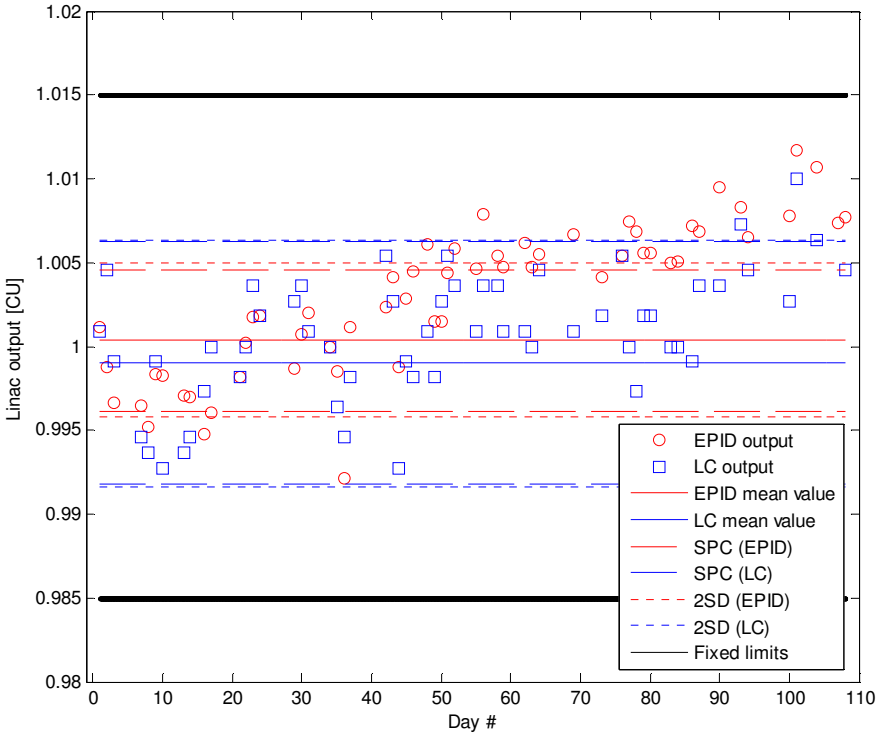

Figure 19. Output average chart for Linacheck daily output measurement for 15 MV and a field size of 10x10 cm2, giving a comparison between SPC limits and limits obtained by calculating the standard deviation. Both limits are obtained by evaluation of the first 20 data points and the SPC limits are obtained by applying statistical process control analysis.

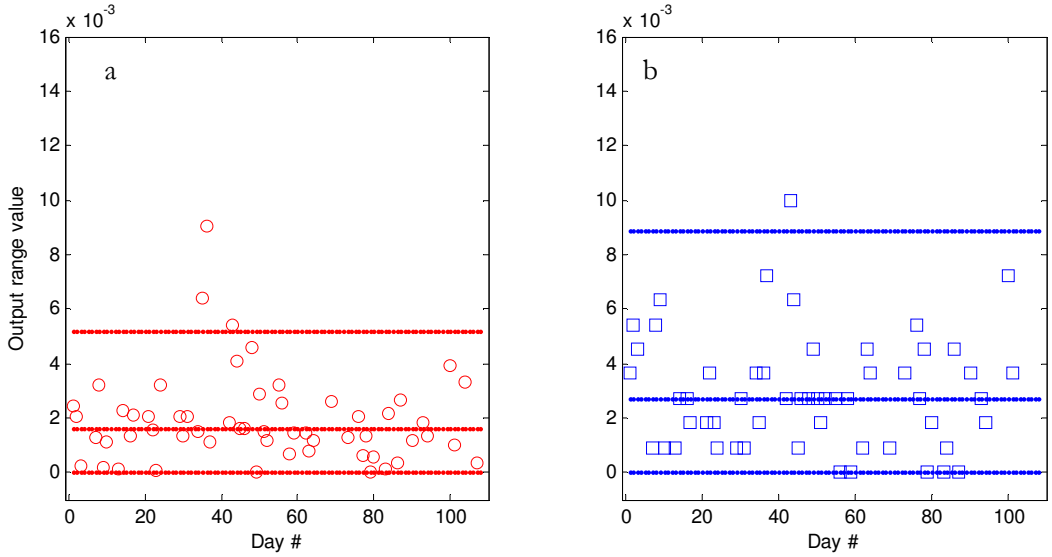

Figure 20. Output range chart for daily output measurements for 15 MV and a field size of 10x10 cm2, carried out with a) EPID and b) Linacheck.

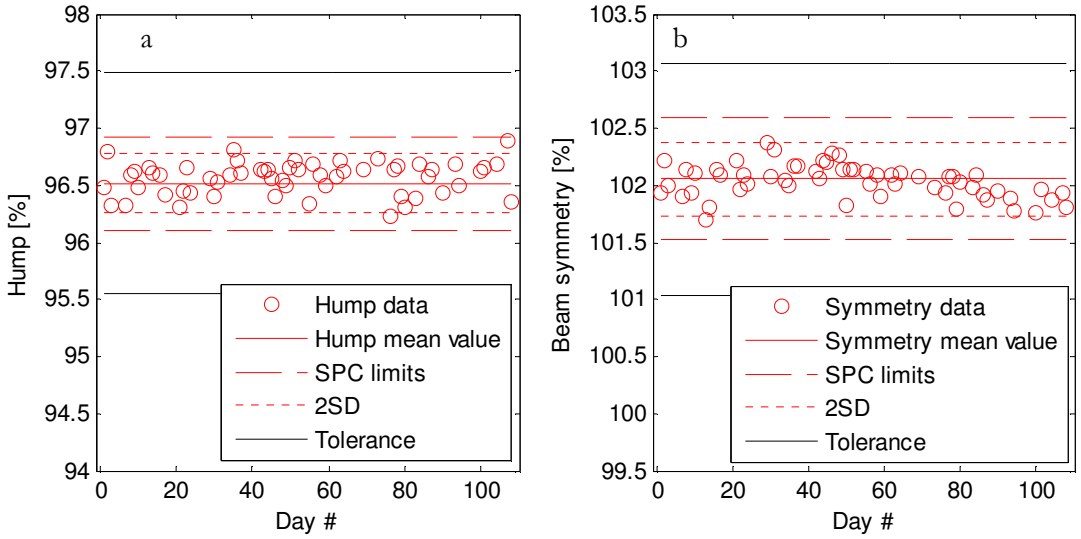

Figure 21. Average chart obtained from daily EPID measurements for 15 MV photons and a field size of 10x10 cm² for a) hump values and b) symmetry values. SPC limits and standard deviation based on the first 20 data points.

Appendix V – Abstract accepted at the 2011 joint AAPM/COMP meeting

Abstract

Purpose: To investigate the suitability of an a-Si EPID as a dosimetric quality assurance device. Action thresholds are obtained using statistical process control (SPC) and introduced known errors detected by the EPID are related to measurements with other quality assurance devices.
Method and Materials: Measurements were performed using a Varian Clinac 2300iX linear accelerator (Varian, Inc., Palo Alto, CA, USA), equipped with an a-Si EPID (Varian aS1000). The suitability of the EPID as a device for daily monitoring of the beam output was investigated for 6MV and 15MV by comparing measurements with the EPID and PTW Linacheck (PTW GmBh, Freiburg, Germany). The ability of an a-Si EPID to verify the beam quality and beam profile parameters was investigated by introducing known errors. A MATLAB© script was developed for analysis of the acquired EPID images. Using statistical process control (SPC), the data was validated and action thresholds were obtained.
Results: The daily measurements with the EPID resulted in good agreement with the PTW Linacheck in detecting output deviations. Obtaining actions thresholds with the use of SPC analysis increased the probability to detect systematic errors in comparison to the use of the mean and standard deviation as primary tools to evaluate the data. Introduced known errors in beam quality and profile parameters could be readily detected by the a-Si EPID and was traceable to water measurements and data collected during commissioning of the linac. A deviation of 1.5% in the TPR measured in water corresponded to a 0.9% change in the hump measured with EPID.
Conclusion: An EPID has proven to be a useful device for daily constancy control of linac output. With the use of SPC one can readily detect systematic errors. Simultaneously it can be utilized as a device to control the constancy of beam quality and beam profile parameters.

Supporting document

Innovation/Impact: This study emphasizes the benefits of utilizing statistical process control (SPC) and electronic portal imaging devices (EPID) for routine quality assurance (QA) of medical linear accelerators. It has been concluded that a QA procedure combining these tools is more practical and not as time consuming in comparison to, for example, the use of PTW Linacheck for daily monitoring of linac output. Evaluation with the use of the SPC concept also increases the possibility to distinguish systematic from random errors in comparison to evaluation using mean and standard deviation.

Quality assurance of linear accelerators is typically performed with the use of a single ion chamber, ion chamber/diode arrays or film. However, the relatively poor resolution of ion chambers and diodes, limitation in field size and the fact that the use of these devices is time consuming as well as cumbersome must be considered. A high resolution amorphous silicon electronic portal imaging device (a-Si EPID) is mounted directly on the linac. In addition to geometric verification of patient position, which the EPID is primarily designed for, it can be useful as a quality assurance device for control of typical machine specific parameters that needs to be monitored on a daily, weekly or monthly basis. Most of the previous work on quality assurance with the use of EPIDs has been carried out using fluoroscopic or liquid-filled ion chamber EPIDs. Work has also been carried out using newer amorphous silicon (a-Si) EPIDs mounted on dual energy Precise linacs (Elekta Oncology Systems, Crawley, UK). The present study differ from previous investigations by being carried out using a Varian Clinac 2300iX linear accelerator (Varian, Inc., Palo Alto,

CA, USA), equipped with an a-Si EPID (Varian aS1000), and by applying statistical process control as primary tool to evaluate the data.

Initially feasibility tests were performed by controlling the linearity between measured output and the prescribed dose between 95 and 105 monitor units (MU) in steps of 1 MU. For 6 MV it can be seen in figure 1 (a) that the EPID has an ability to distinguish deviations in output similar to the ability of a routinely used ionization chamber (FC65-P, Scanditronix Wellhöfer, Uppsala, Sweden) (figure 1 (a)). Feasibility tests also included checking the output constancy when measured with the EPID. Measuring several times for the same settings resulted in a standard deviation of less than 0.1%. The conclusion from the feasibility tests was that the EPID should be suitable as a device for quality assurance of medical linear accelerators. It could also be concluded that utilizing the SPC concept makes the QA system more sensitive to deviations from the baseline values. The thresholds obtained by the SPC analysis spans over a much narrower gap in linac output and one could therefore detect possible systematic errors at an earlier stage when compared to the usage of thresholds obtained by the mean and standard deviation.

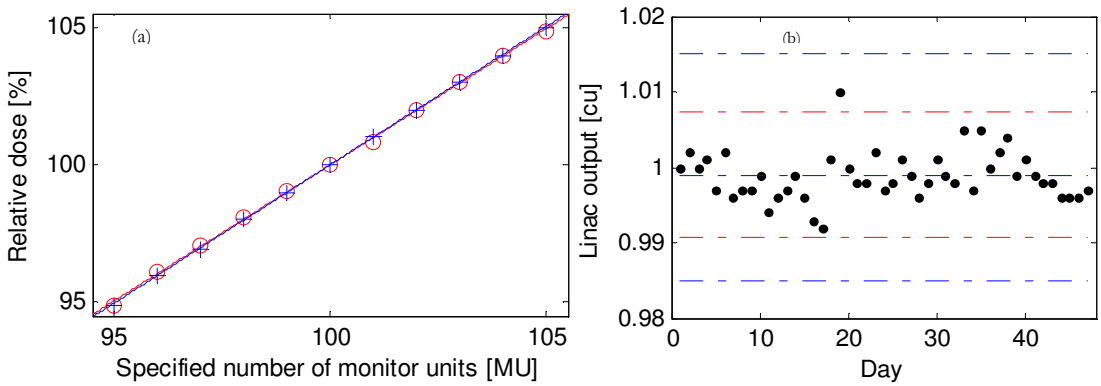

Figure 1. *(a) Relative dose as a function of specified number of MU for EPID (red) and water (blue) measurements (b) evaluation of daily QA data (black dots) using thresholds obtained with SPC analysis (red dashed) and mean and standard deviation (blue dashed).*

To further analyze the ability of the EPID to act as a quality assurance device known errors was introduced. Initially the bending current shunt voltage was varied so that a significant change in beam quality could be detected by measuring a depth dose curve in water. With the known error in beam quality maintained measurements were performed with the EPID (see figure 2 (a)). The results could then be compared between the different devices and the result suggests that EPID also can be used to monitor the beam energy by calculating the hump. Hump is, according to International Electrotechnical Commission (IEC), defined as

$$\text{Hump} = \frac{(D_R + D_L)}{2 \cdot D_C} \cdot 100,$$

where D_L and D_R are the left and right extreme values of the flattened area and D_C is the signal at the beam centre.

Table 1. The effects of introduced known error in beam energy on the TPR measured with an ionization chamber (CC13, Scanditronix Wellhöfer, Uppsala, Sweden) in a 3D water phantom (Blue phantom, Scanditronix Wellhöfer, Uppsala, Sweden), the hump measured with EPID and the hump measured with Starcheck.

Measurement device	Blue phantom (TPR)	EPID (Hump) [%]	Starcheck (Hump) [%]
Before beam energy adjustment	0.669	96.9	95.3
After beam energy adjustment	0.659	97.7	95.9
Change [%]	-1.5	0.9	0.6

The ability of the EPID to detect changes in the beam profile was also tested by changing the steering current (see figure 2 (b)). In this case the symmetry and flatness was calculated using the IEC definitions as below.

$$\text{Symmetry} = \left(\frac{D_L}{D_R}\right)_{Max} \cdot 100 \qquad \text{Flatness} = \left(\frac{D_{Max}}{D_{Min}}\right) \cdot 100$$

Table 2. Effect of introduced known error in steering current on symmetry calculated from measurements with EPID, diode (PFD-3G, IBA dosimetry, Uppsala, Sweden) in water (Blue phantom), Starcheck and the T-sym parameter on the linac.

Measurement device	EPID	Blue phantom	Starcheck	T-sym [V]
Before beam profile adjustment [%]	100.6	101.2	101.4	0.0
After beam profile adjustment [%]	103.3	115.9	103.5	-2.2
Change [%]	2.7	14.6	2.1	-

From the results presented in table 1 it can be concluded that there exist traceability between the different measuring systems. Where a change in beam quality for example could be seen as a 1.5% change in TPR when measured in water, a 0.9% change could also be detected in hump when the EPID was used. Similar conclusions can be drawn, evaluating the profile measurements (table 2). A change in the crossline symmetry (transverse symmetry, T-sym parameter) on the linac from 0 to approximately -2 V could be detected as a 14.6% change in the symmetry when measured in water and a change of 2.7% and 2.1% as measured with EPID and Starcheck, respectively. Note that an interlock would normally interrupt the machine if the T-sym parameter exceeds a value of ±2 V. The fact that smaller changes in symmetry are detected with the EPID in comparison to the measurements in water can be attributed to the lack of build up on the EPID. However, the detected change in symmetry is in the same order as the change detected with the Starcheck (where build up material was used) and one can from the results relate the detected deviation with the EPID to measurements in water. The results presented in this supporting document include only a photon beam of 6 MV and a field size of 25x25 cm². The study has however shown similar results for a field size of 10x10 cm² and also for both field size with 15 MV. It should be noted that measurements also were performed with the same settings as during the commissioning of the accelerators and the results are therefore also traceable back to the baseline values of the beam quality as well as beam profile parameters.

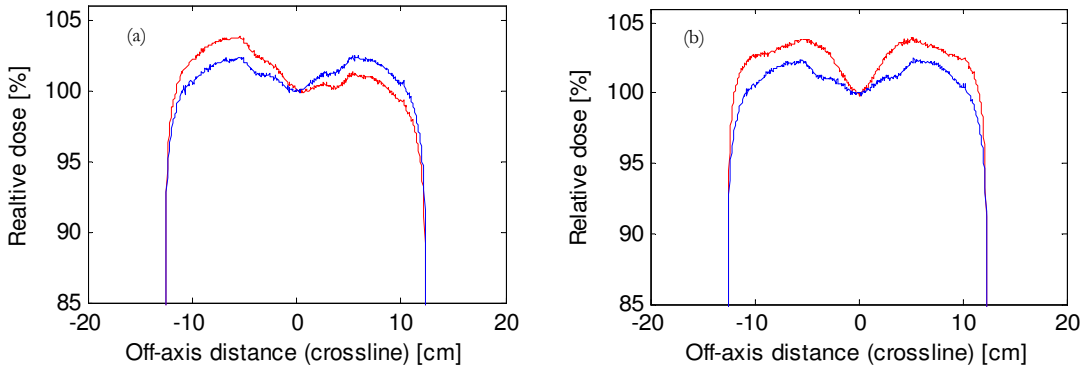

Figure 2. *(a) Beam profiles for original (blue) and with introduced asymmetry (red) measured with EPID (b) beam profiles for original (blue) and with decrease in beam energy (red) measured with EPID.*

LUND
UNIVERSITY